Basic Sciences

Principles and Practice of Ophthalmology

DANIEL M. ALBERT, M.D.
Frederick A. Davis Professor and Chairman,
Department of Ophthalmology,
University of Wisconsin Medical School,
Madison, Wisconsin

FREDERICK A. JAKOBIEC, M.D., D.Sc.(Med.)
Henry Willard Williams Professor of Ophthalmology,
Professor of Pathology, and Chairman,
Department of Ophthalmology,
Harvard Medical School;
Chief, Department of Ophthalmology, and
Surgeon in Ophthalmology,
Massachusetts Eye and Ear Infirmary,
Boston, Massachusetts

NANCY L. ROBINSON, A.B.
Managing Editor

W.B. SAUNDERS COMPANY
A Division of Harcourt Brace & Company
Philadelphia London Toronto Montreal Sydney Tokyo

105. Rodieck RW: The primate retina. *In* Steklis HD, Erwin J (eds): Comparative Primate Biology. Neurosciences, 4th ed. New York, Alan R Liss, 1988, pp 203–278.
106. Schiller PH, Malpeli JG: Properties and tectal projections of monkey retinal ganglion cells. J Neurophysiol 40:428, 1977.
107. Simpson JI: The accessory optic system. Annu Rev Neurosci 7:13, 1984.
108. Wässle H, Peichl L, Boycott BB: Dendritic territories of cat retinal ganglion cells. Nature 292:344, 1981.
109. Canzek V, Wolfsenberger M, Amsler U, Cuenod M: In vivo release of glutamate and aspartate following optic nerve stimulation. Nature 293:572, 1981.
110. Tsai G, Stauch BL, Vornov JJ, et al: Selective release of N-acetylaspartylglutamate from rat optic nerve terminals in vivo. Brain Res 518:313, 1990.
111. Kuljis RO, Karten HJ: Neuroactive peptides as markers of retinal ganglion cell populations that differ in anatomical organization and function. Vis Neurosci 1:73, 1988.
112. Brecha NC, Eldred W, Kuljis RO, Karten HJ: Identification and localization of biologically active peptides in the vertebrate retina. *In* Osborne NN, Chader G (eds): Progress in Retinal Research, vol. 3. Oxford, Pergamon, 1984, pp 185–226.
113. Brecha N, Hendrickson A, Floren I, Karten HJ: Localization of substance P-like immunoreactivity within the monkey retina. Invest Ophthalmol 23:147, 1982.
114. Curcio CA, Hendrickson A: Organization and development of the primate photoreceptor mosaic. *In* Osborne NN, Chader G (eds): Progress in Retinal Research, vol. 10. Oxford, Pergamon, 1982, pp 89–120.
115. Boycott BB, Dowling JE: Organization of the primate retina: Light microscopy. Philos Trans R Soc Lond [B] 255:109, 1969.
116. Famiglietti EV, Kolb H: A bistratified amacrine cell and synaptic circuitry in the inner plexiform layer of the retina. Brain Res 84:293, 1975.
117. Dacheux RF, Raviola E: The rod pathway in the rabbit retina: A depolarizing bipolar and amacrine cell. J Neurosci 6:331, 1986.
118. Peichl L, Ott H, Boycott BB: Alpha ganglion cells in mammalian retinae. Proc R Soc Lond [B] 231:169, 1987.

Chapter 24

Müller Cells and the Retinal Pigment Epithelium

ERIC A. NEWMAN

INTRODUCTION

Nonneuronal Retinal Cells

Müller cells and retinal pigment epithelium cells are the two principal nonneuronal cells of the retina. Unlike retinal neurons, they do not appear to participate directly in the transfer or processing of visual information. They are, however, intimately involved in retinal function and exert a profound influence on the behavior of retinal neurons.

Müller cells are the principal glial cells of the neural retina. As such, they are believed to assume many of the functions of astrocytes and oligodendrocytes, the two major classes of glial cells that are found in other brain regions but are largely absent from the retina. (Astrocytes are present in the nerve fiber layer of the mammalian retina but are absent from deeper retinal laminae.) Müller cells participate in the regulation of the extracellular environment in the retina, buffering light-evoked variations in extracellular K^+ concentration ($[K^+]_O$) and removing neurotransmitters from synapses by active uptake. Müller cells are also thought to provide structural and metabolic support to retinal neurons and may regulate CO_2 levels within the neural retina.

Retinal pigment epithelium (RPE) cells, the other major class of nonneuronal retinal cells, form a cuboidal epithelial layer that lies between the photoreceptors and the choroidal circulation. Like other epithelia, the RPE functions to transport ions and fluid and constitutes a barrier that forms an essential component of the blood-retinal barrier. The RPE cells also participate in the renewal of photoreceptor outer segments and play a vital role in the metabolism and reisomerization of retinoids, which are an essential component of the photoreceptor photopigments.

Müller cells and retinal pigment epithelium cells share many features and properties. The processes of both cells envelop retinal neurons, with RPE cells covering the photoreceptor outer segments and Müller cells surrounding all other types of retinal neurons. Both cells have a high K^+ permeability and generate transretinal voltages in response to light-evoked variations in $[K^+]_O$. Indeed, the response of Müller cells and RPE cells to a light-evoked $[K^+]_O$ decrease generated by the rods leads jointly to the generation of the c-wave of the electroretinogram (ERG).

Development of Nonneuronal Cells

Müller cells and RPE cells, together with the retinal neurons, share a common developmental origin. As is discussed in *Principles and Practice of Ophthalmology: Clinical Practice,* Chapter 188, the primary optic vesicle of the fetal eye forms from an outbudding of the primitive neural tube.[1, 2] A secondary invagination of the optic vesicle forms the optic cup. At early stages, the optic cup consists of two epithelial layers separated

by a fluid-filled space that is initially continuous with the brain ventricles. This space develops into the subretinal space that separates photoreceptors from the RPE in the mature retina.

The outer cell layer of the optic cup retains its epithelial nature as the eye matures. It remains only a single cell thick and differentiates into the RPE. The inner cell layer of the optic cup, in contrast, undergoes profound differentiation and develops into a multilayered neural tissue containing many distinct types of cells. It loses most vestiges of its original epithelial origin.

Müller cells of the neural retina, however, do retain some features reminiscent of their origin in the inner epithelial layer of the optic cup. Like epithelial cells, Müller cells span the entire width of the neural retina. These cells also have distinct basal and apical surfaces. The basal surface terminates at the inner (proximal) border of the retina and forms a basal lamina, the inner limiting membrane of the retina. The apical end of the cell, in contrast, is composed of microvilli that project into the subretinal space. Like the RPE and other epithelial cells, Müller cells have ion channels and transport systems that are localized to specific cell regions.

Scope of Chapter

This chapter describes the principal functions of Müller cells and retinal pigment epithelium cells as well as the morphologic and physiologic features that underlie these functions. The membrane properties of these cells, including ion channel and transport mechanisms, are stressed, since they are the basis of many of the functions of both Müller cells and the RPE.

Müller cells and the RPE generate several components of the electroretinogram. The physiologic mechanisms responsible for the generation of these responses are discussed herein. A detailed description of ERG generation and phenomenology is not included in this chapter, however, as they are described in detail in Chapter 25. Two important functions of the RPE, phagocytosis of photoreceptor outer segments and retinoid metabolism and isomerization, are covered in detail in Chapter 19 and are discussed only briefly here.

Owing to space limitations, this chapter does not cover Müller cells and the RPE exhaustively. The reader is referred to other recent reviews of Müller cells[3–6] and the retinal pigment epithelium[6–10] for additional information.

MÜLLER CELLS

Müller cells are the principal glial cells of the retina. They are oriented radially within the neural retina, extending from the photoreceptor inner segments to the vitreal border of the retina. Throughout most of the retina, Müller cells are the sole type of glial cells present (excluding microglia). Oligodendrocytes, which are the myelin-forming glial cells of the central nervous system (CNS), are completely absent in the primate retina (which is devoid of myelinated fibers). Astrocytes, the second major class of glia in the CNS, are found only at the proximal border of the mammalian retina in the nerve fiber and ganglion cell layers.

Because of the absence of astrocytes and oligodendrocytes from the retina, Müller cells are thought to assume many of their functions. These include (1) regulation of extracellular ion levels (K^+ and perhaps other ions), (2) active uptake of neurotransmitters (glutamate, γ-aminobutyric acid [GABA]), (3) structural and metabolic support of neurons, and (4) neuronal guidance during development. Müller cells also generate several components of the ERG and may participate in the regulation of CO_2[11] and in the visual cycle of retinoid metabolism in the retina.[10, 12]

Structure

Müller cells span almost the entire depth of the neural retina (Fig. 24–1). The distal ends of these cells extend past the outer limiting membrane at the level of the photoreceptor inner segments, whereas their proximal ends form the inner limiting membrane at the vitreal-retinal border. Müller cell somata lie in the inner nuclear layer. The general morphology of Müller cells has been described in light and electron microscopic studies.[13–19]

Microvillar processes on the distal (apical) end of

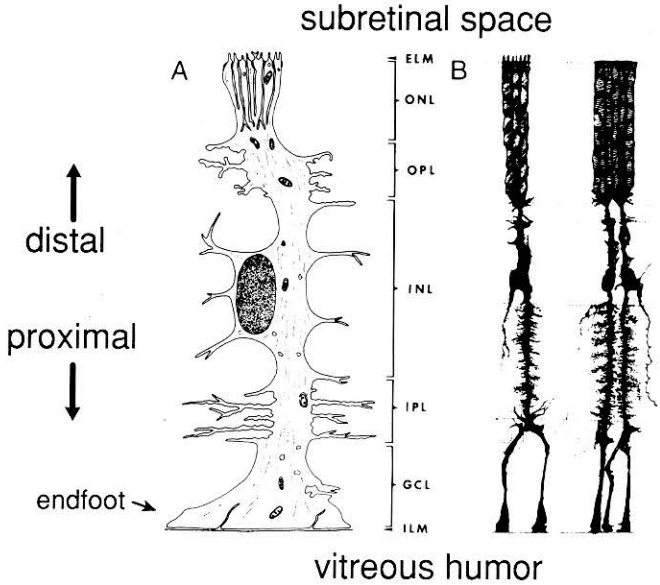

Figure 24–1. Müller cells of the mudpuppy *(A)* and the ox *(B)*. The mudpuppy drawing is based on electron microscopic observations, while the ox cells are from Golgi-stained material. Visible in cells of both species are microvilli at the outer limiting membrane, the soma in the inner nuclear layer, processes extending tangentially in most retinal layers, and one or more endfeet at the inner limiting membrane. ELM, outer (external) limiting membrane; ONL, outer nuclear layer; OPL, outer plexiform layer; INL, inner nuclear layer; IPL, inner plexiform layer; GCL, ganglion cell layer; ILM, inner limiting membrane. (Modified from Miller RF, Dowling JE: Intracellular responses of the Müller (glial) cells of mudpuppy retina. J Neurophysiol 33:323, 1970; and Ramon y Cajal S: The Structure of the Retina. Springfield, IL, Charles C Thomas, 1972.)

Müller cells project past the outer limiting membrane into the subretinal space. These microvilli increase the surface area in this cell region and are implicated in the exchange of metabolites and ions between Müller cells and the subretinal space.

Lying just proximal to the Müller cell microvilli are a series of junctional complexes between adjacent Müller cells and between Müller cells and photoreceptors.[18] In mammals, these complexes consist primarily of zonulae adherentes.[20, 21] The gap junctions present in lower vertebrates[17, 18] mediate electrical coupling between adjacent Müller cells.[22, 23] When viewed through the light microscope, these complexes appear to form a continuous membrane, the outer limiting membrane. In reality, this "membrane" is not a continuous structure and does not represent a barrier to current flow or the diffusion of small molecules.[24]

Within the neural retina, many fine processes extend from the central shaft of Müller cells into the spaces between neurons. These processes cover most, but not all, neuronal surfaces. In the nuclear layers, these processes surround neuronal somata and have the appearance (in dye-filled cells) of an extensive network of fingers surrounding hollow spheres. In the plexiform layers, Müller cell ramifications are even more extensive, covering most dendritic processes of neurons and extending up to synaptic clefts. In primates, Müller cell processes come in direct contact with most axons in the nerve fiber layer.[25, 26]

Blood vessels within the retina are completely surrounded by processes of glial cells.[20, 27] Vessels deep within the retina (those lying at the inner and outer margins of the inner nuclear layer) are surrounded by Müller cell processes. The more superficial blood vessels (those at the vitreal surface and in the ganglion cell layer) are surrounded by the processes of both Müller cells and astrocytes. In all cases, a basal lamina lies between the glial cell processes and the blood vessels.

The proximal (basal) end of the Müller cell is terminated by the cell endfoot. The endfoot lies immediately adjacent to the inner limiting membrane, which in reality is the basal lamina formed by this portion of the cell.

Freeze-fracture studies reveal that a distinct type of intramembrane particle is localized to the endfeet of Müller cells.[20, 28, 29] These "orthogonal arrays of particles" (OAPs; also termed "assemblies") are composed of rectilinear particle arrays. The OAPs are also present on Müller cell processes contacting blood vessels in the inner nuclear layer.[30] The function of OAPs is not known, but they could represent K^+ channels,[31] which are also localized preferentially to the cell endfoot (see below). Astrocytic glial cells also contain OAPs, where they are localized to cell endfeet.[32, 33]

Most glucose stored within the retina in the form of glycogen is localized to Müller cells.[17] Glycogen granules are prevalent in Müller cells of nonvascularized retinae and somewhat less so in species with a retinal circulation.[34, 35] Retinae that can quickly extract glucose from the blood (those with an extensive vascularization) apparently do not need large stores of glucose.

Immunocytochemical studies demonstrate that Müller cells contain cellular retinol-binding protein (CRBP) and cellular retinal-binding protein (CRalBP),[36, 37] two molecules that bind visual cycle retinoids (see below). The two proteins also are present in the RPE, where they are intimately involved in retinoid metabolism and isomerization. The presence of these proteins within Müller cells raises the interesting possibility that this glial cell may also be a direct participant in the visual cycle.[10]

Membrane Physiology

A great deal is known about the membrane properties of Müller cells. Much of this information comes from experiments on freshly dissociated cells. Amphibian species have been used most widely, but mammals, including primates, have also been studied.

CELL MEMBRANE POTENTIAL

Like other glial cells, the resting membrane potential of Müller cells is very large, approximately −80 to −95 mV.[18, 38, 39] This potential is more negative than those of retinal neurons. The membrane potential of photoreceptors, for instance, is ~ −40 mV, whereas that of ganglion cells is −60 to −70 mV.

The large resting potential of Müller cells is directly attributable to their selective permeability to K^+. Like astrocytes and oligodendrocytes, Müller cells are almost exclusively permeable to K^+. The cells behave as almost ideal K^+ electrodes, with the cell membrane potential determined by the K^+ equilibrium potential

$$K_{equilibrium}\ (mV) = -58 \log \left(\frac{[K^+]_i}{[K^+]_o} \right) \quad (1)$$

For a 10-fold increase in $[K^+]_o$, Müller cells depolarize almost 58 mV.[23, 40] This behavior demonstrates that Müller cell permeability to ions other than K^+ is extremely low. In frog Müller cells, for instance, the resting permeability to Na^+ is only ~0.2% that of the K^+ permeability.[40]

Müller cells are not only selectively permeable to K^+, they also have a very high K^+ conductance, which results in a low cell input resistance. Cell resistance ranges from 4 to 21 MΩ in different species.[39] Retinal neurons, in contrast, have an input resistance as high as 1000 MΩ or more.

ION CHANNELS

Inward-Rectifying K^+ Channel

The large K^+ conductance of Müller cells results from the large number of inward-rectifying K^+ channels on the cell surface. These inward-rectifying K^+ channels are open and conduct current at the normal resting potential of the cell. Most other ion channels (including other K^+ channels), in contrast, are closed at a membrane potential of −80 mV and only open when cells are depolarized.

The inward-rectifying K^+ channel of Müller cells has been characterized in voltage-clamp studies (Fig. 24–2). The current/voltage relation of salamander Müller cells, measured by whole-cell voltage-clamp of cells bathed in high $[K^+]_o$, shows strong inward rectification; much larger currents are evoked when cells are hyperpolarized than when they are depolarized.[41] This current/voltage relation has the same form for intact cells and for cells missing their endfeet, indicating that the same inward-rectifying channels are found in all cell regions.[41] Similarly, cell-attached membrane patches from the Müller cell soma and endfoot have almost identical inward-rectifying current/voltage relations.[41] The inward-rectifying conductance of Müller cells is blocked effectively by micromolar concentrations of Ba^{2+}.[42]

Single-channel recordings from dissociated cells also demonstrate that an inward rectifier is the predominant channel in Müller cells. In recordings from Müller cell membrane patches, inward-rectifying channels are observed most frequently.[43] For hyperpolarizing voltages, the unitary conductance of this channel is in the range of 20 to 30 pS in different species[41, 43, 44] (with high external $[K^+]_o$). As discussed below, the voltage- and $[K^+]_o$-dependent properties of the inward-rectifying channel facilitates Müller cell regulation of light-evoked variations in $[K^+]_o$.

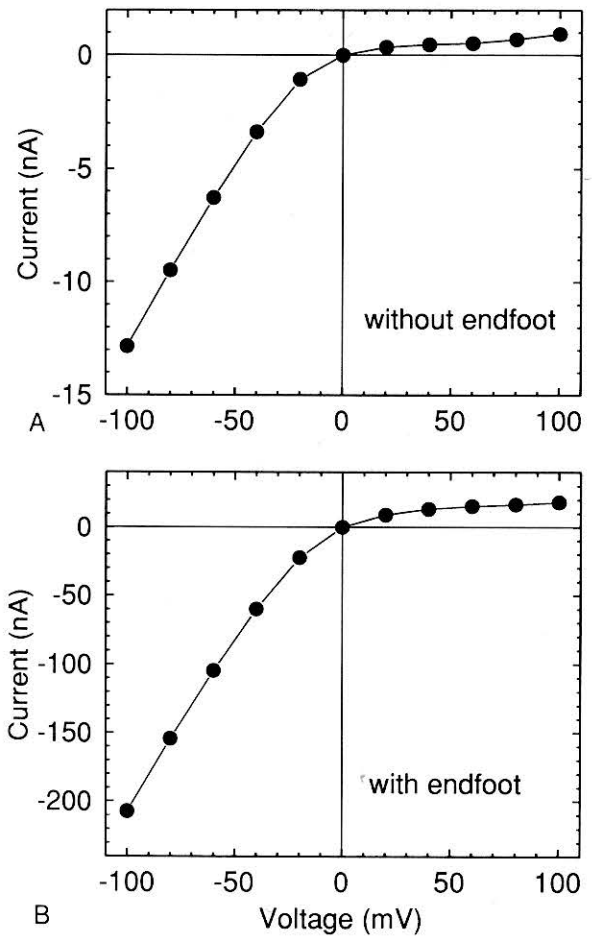

Figure 24–2. Current/voltage (I/V) relations of two dissociated salamander Müller cells, one with its endfoot missing *(A)* and a second with its endfoot intact *(B)*. The two cells show nearly identical inward-rectifying properties, indicating that membrane conductance in all cell regions is mediated by inward-rectifying K^+ channels. Currents are much larger for the cell with its endfoot, indicating that most channels are localized to the endfoot region. Results are from two-electrode voltage-clamp recordings with 88 mM K^+ in both internal and external solutions.

Distribution of K^+ Channels

The K^+ channels of Müller cells are distributed in an extremely nonuniform manner over the cell surface. In amphibian Müller cells, for instance, almost all of the input conductance is contained in the cell endfoot. Dissociated salamander cells that are lacking their endfeet have a cell conductance that is only ~5% of the conductance of cells with their endfeet intact.[40, 45] This indicates that ~95% of the total conductance of the cell is localized to the endfoot.

K^+ channel distribution has also been determined by monitoring cell depolarizations as $[K^+]_o$ is raised over small regions of the cell surface. In amphibians, ejecting a high $[K^+]$ solution onto the cell endfoot evokes far larger depolarizations than do K^+ ejections onto other cell regions,[40] indicating that most K^+ channels are located at the endfoot.

This finding has been confirmed in cell-attached patch-clamp studies of dissociated salamander Müller cells. Membrane patches on the cell soma generally contain only a few K^+ channels, whereas patches on the endfoot contain up to 600 channels.[41, 43] Patch-clamp studies have also confirmed that the same type of K^+ channel (the K^+ inward-rectifying channel) is found in all cell regions. K^+ conductance is localized to the endfoot simply because there is a much higher density of channels in this cell region.

The distribution of K^+ channels in mammalian Müller cells is more complex than it is in amphibians and is thought to be related to the degree of retinal vascularization in different species (Figs. 24–3 and 24–4). In mammalian species with nonvascularized retinae, such as the rabbit and guinea pig, K^+ conductance is largest at the cell endfoot, as it is in amphibians.[39, 46] In species with vascularized retinae, however, other cell regions also display high K^+ conductance. In mice and monkeys, the largest K^+ conductance is found near the cell soma rather than at the endfoot.[39] And in the cat, K^+ conductance is largest at the distal (photoreceptor) end of the cell.

Blood vessels in the inner nuclear layer of mammalian retinae are completely surrounded by Müller cell processes.[20, 27] This is precisely the retinal region in which mammalian Müller cells have the highest K^+ conductance. This correspondence suggests that the cell processes that contact blood vessels have high K^+ conductance, as do the endfeet at the inner limiting membrane.[39] Because of this similarity in membrane properties, the processes in contact with blood vessels should perhaps be considered endfeet themselves. As described above, these processes also share morphologic similarities with the vitreal endfeet (a basal lamina and high densities of OAPs).

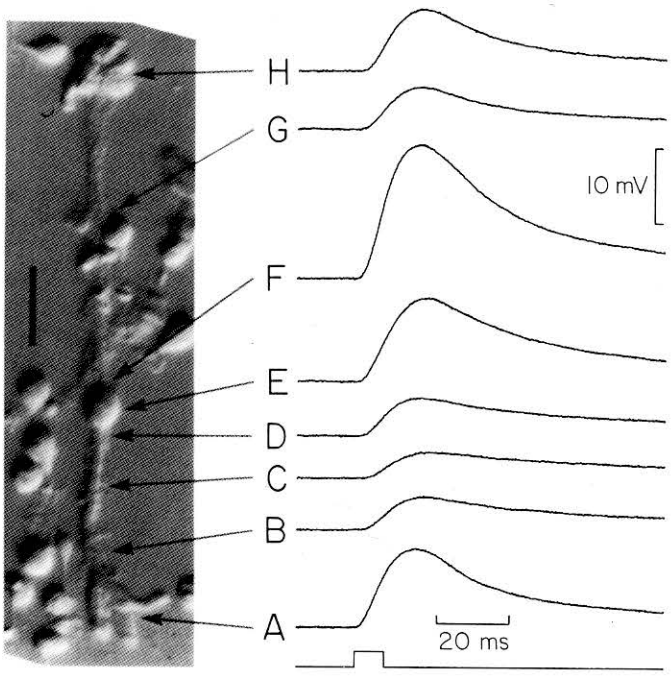

Figure 24–3. Voltage responses of a dissociated owl monkey Müller cell to focal K^+ ejections. Responses recorded from the cell pictured at left. Large depolarizations are evoked when K^+ is pressure-ejected onto the endfoot (A) and onto the soma (E and F), demonstrating that these cell regions have a high density of K^+ channels. Scale bar = 20 μm. (From Newman EA: Distribution of potassium conductance in mammalian Müller (glial) cells: A comparative study. J Neurosci 7:2423, 1987.)

Other Ion Channels

Müller cells have a full complement of voltage-dependent ion channels in addition to the K^+ inward rectifier. Whole-cell voltage-clamp studies of amphibian Müller cells demonstrate the presence of Ca^{2+} channels, Ca^{2+}-activated K^+ channels, and fast-inactivating (A type) K^+ channels.[47] When the K^+ conductance of salamander Müller cells is blocked (a decidely nonphysiologic state), the Ca^{2+} channels are able to generate Ca^{2+} action potentials.[47] Ca^{2+}-activated K^+ channels and several types of large conductance K^+ channels have also been observed in patch-clamp studies of rabbit Müller cells[48] and cultured retinal glial cells.[49]

Ca^{2+}, Ca^{2+}-activated K^+, and type A K^+ channels do not open appreciably until the cell membrane potential is depolarized to between −60 and −40 mV. However, the resting membrane potential of Müller cells is −80 to −95 mV, and under normal physiologic conditions cells never depolarize more than 5 or 10 mV.[18, 38, 50, 51] Thus, it seems unlikely that these three types of channels open or conduct current in vivo and their function in Müller cells remains unclear.

TRANSPORT SYSTEMS

Müller cells possess a HCO_3^- transport system and a Na^+/K^+-ATPase that have been characterized in some detail. These transport systems are described in this section. In addition, Müller cells have active uptake systems for several neurotransmitters. These systems are discussed below.

Na^+/HCO_3^- Cotransporter

Müller cells have an electrogenic Na^+/HCO_3^- cotransport system that transports both HCO_3^- and Na^+, along with a net negative charge, across the cell membrane. The cotransporter has been characterized in a voltage-clamp study utilizing dissociated amphibian Müller cells.[11, 52] In this preparation, an increase in $[HCO_3^-]_o$ evokes a cell hyperpolarization, the result of the influx of negatively charged HCO_3^-. The cotransporter in salamander Müller cells has a stoichiometry of ~3:1; 3 HCO_3^- are transported along with a single Na^+. The Na^+/HCO_3^- cotransporter is Na^+ dependent, Cl^- independent, and is inhibited by disulfonic stilbenes DIDS and DNDS and by harmaline.[11, 52] To date, the cotransporter has only been studied in amphibians and fish[52, 53]; mammalian cells have not been investigated.

Na^+/HCO_3^- cotransport sites are distributed nonuniformly over the cell surface in salamander Müller cells. Like K^+ channels, they are concentrated preferentially in the cell endfoot.[11] It has been suggested[11] that this asymmetric distribution of cotransporter sites could function to regulate CO_2 levels in the retina, perhaps helping to buffer light-evoked variations in pH_o.[54, 55] Carbonic anhydrase, which is found in high levels within Müller cells,[56, 57] will convert CO_2 to HCO_3^- within the

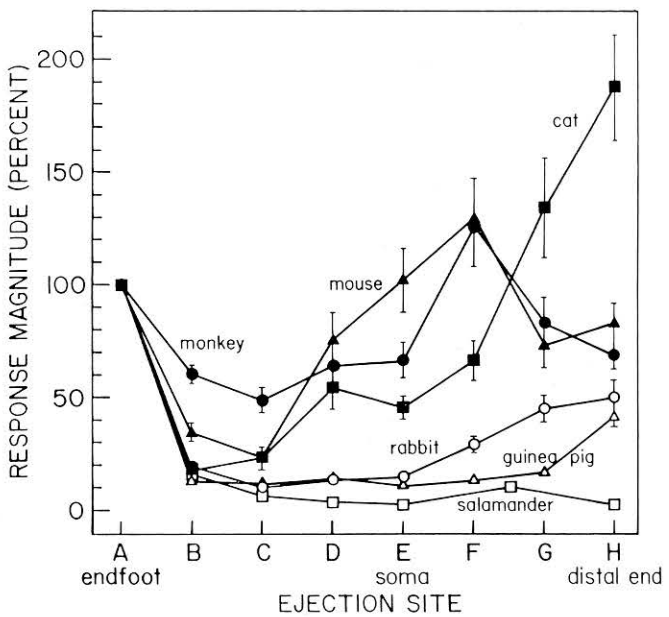

Figure 24–4. Summary of voltage responses to K^+ ejections recorded from dissociated Müller cells of the salamander (□), rabbit (○), guinea pig (△), mouse (▲), owl monkey (●), and cat (■). Response magnitude (normalized to endfoot responses) is plotted as a function of ejection site location. In species with avascular retinas (salamander, rabbit, guinea pig), K^+ channel density is highest at the endfoot. In species with vascularized retinas (mouse, monkey, cat), channel density is highest near the soma or at the distal end of the cell. (From Newman EA: Distribution of potassium conductance in mammalian Müller (glial) cells: A comparative study. J Neurosci 7:2423, 1987.)

cells. The HCO_3^- will be transferred out of the cell through the Na^+/HCO_3^- cotransport system at the endfoot, directly into the vitreous humor. This CO_2 homeostatic mechanism may prove to be an important function of Müller cells, but this remains to be verified experimentally.

Na^+/K^+-ATPase

Müller cells, like other cells, have an Na^+/K^+-ATPase that serves to maintain transmembrane Na^+ and K^+ gradients. The Na^+/K^+ pump in Müller cells is electrogenic and helps to maintain the cell resting potential; when cells are poisoned with the pump inhibitor ouabain, there is a rapid cell depolarization of a few millivolts (inhibition of the electrogenic pump), followed by a slower steady depolarization (a running down of the transmembrane K^+ gradient).[40, 58]

The distribution of the Na^+/K^+-ATPase over the surface of Müller cells has been determined in ouabain-binding studies. In both the rabbit[59] and turtle,[60] the Na^+/K^+ pump is localized preferentially to the microvilli at the distal end of the cell and to processes within the plexiform layers. The activity of the Na^+/K^+-ATPase in rabbit Müller cells varies as a function of $[K^+]_O$ and increases for $[K^+]_O$ values up to 10 mM.[61] The expression of distinct isozymes of the catalytic subunit of the pump in Müller cells and retinal neurons differ[62] and may account for the uncommon $[K^+]_O$ dependence of the pump in Müller cells.

NEUROTRANSMITTERS

Glutamate Transport

An electrogenic glutamate uptake system has been characterized in amphibian Müller cells. The system transports a single glutamate along with $3Na^+$ into Müller cells when glutamate concentration is raised extracellularly. As in astrocytes, high-affinity glutamate uptake is believed to play an important role in the removal of the neurotransmitter, and thus the termination of synaptic transmission, at glutamatergic synapses.

Raising external glutamate concentration results in glutamate influx via the transport system and in cell depolarization.[63–65] The glutamate transport system is localized preferentially to the distal half of Müller cells. Ejection of glutamate onto the soma or distal end of the cell evokes larger currents than does ejection onto the endfoot.[63] The affinity constant for glutamate binding to the transporter, measured physiologically, is 5 to 20 μM.[65–67]

Glutamate transport is Na^+ dependent; removal of external Na^+ results in almost complete inhibition of the transporter.[63, 65] It has also been suggested that the transporter is modulated by internal K^+ and that removal of internal K^+ abolishes transport.[66, 67] However, other studies indicate that glutamate transport is independent of $[K^+]_i$.[65] Glutamate uptake into Müller cells has also been observed using autoradiographic techniques.[68]

Müller cells have high levels of glutamine synthetase,[69, 70] an enzyme that catalyzes the conversion of glutamate and ammonia to glutamine. This enzymatic reaction serves to maintain low internal glutamate concentrations, assuring that the transport system will continue to pump glutamate into Müller cells when external levels are raised. Thus, external glutamate can be maintained at an extremely low concentration. Glutamine produced by Müller cells is presumably recycled back to glutamatergic neurons, where it is converted back to glutamate.[71]

Other Transmitters

γ-Aminobutyric acid is also transported into Müller cells by a high-affinity uptake system.[68, 72] The GABA transporter, like the glutamate uptake system, is thought to aid in the termination of synaptic transmission by removal of the transmitter from the region of the synaptic cleft. Once GABA is transported into Müller cells, it is metabolized by the enzyme GABA transaminase,[70] the first enzyme in the degradative pathway for GABA. Müller cells lack glutamate decarboxylase, the GABA synthetic enzyme.[70, 73] The degradative enzyme acetylcholinesterase has also been identified in Müller cells.[70]

$GABA_A$ Channel

Müller cells depolarize when exposed to GABA. This response is mediated by the opening of $GABA_A$, ligand-gated chloride channels.[74] The GABA-evoked depolarizing response, which contrasts with the hyperpolarizing response of most neurons, occurs because Müller cells, like other glial cells, have a Cl^- equilibrium potential that is more positive than the cell resting potential.

The GABA-gated channel has been characterized in electrophysiologic studies utilizing dissociated skate Müller cells.[74] The channel has a reversal potential that varies as a function of $[Cl^-]_O$ and closely matches the Cl^- equilibrium potential, demonstrating that the channel is selectively permeable to this anion. The response is half-maximal at ~1 μM GABA and is inhibited by $GABA_A$ antagonists. As has been suggested in other glial systems,[75] such GABA-gated chloride channels may buffer $[Cl^-]_O$ levels in the neighborhood of GABAnergic neuronal synapses.

Light-Evoked Responses

$[K^+]_O$ VARIATIONS

The light-evoked responses of Müller cells are driven largely by variations in $[K^+]_O$. Depolarizing retinal neurons release K^+ into the interstitial space, leading to an increase in $[K^+]_O$. Hyperpolarizing cells (principally the photoreceptors), in contrast, generate a K^+ influx and a reduction in $[K^+]_O$. The $[K^+]_O$ increases and decreases directly modulate the Müller cell membrane potential, which, as we have seen, is determined by the K^+ equilibrium potential.

Light-evoked variations in $[K^+]_O$ within the retina have been measured with K^+-selective microelectrodes

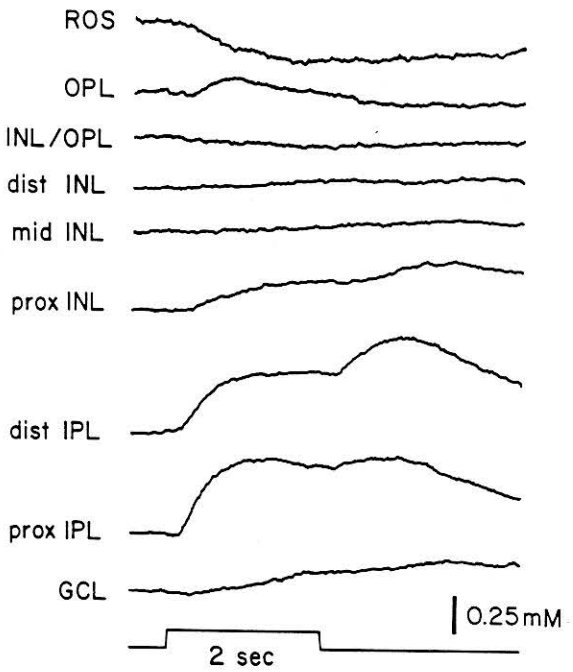

Figure 24–5. Light-evoked variations in $[K^+]_o$ in the frog retina (retinal slice preparation) recorded with K^+-selective microelectrodes. Large $[K^+]_o$ increases are seen in the inner plexiform layer (IPL) at both light onset and offset. A smaller $[K^+]_o$ increase occurs in the outer plexiform layer (OPL) at light onset. A $[K^+]_o$ decrease is present in the subretinal space. ROS, rod outer segments. (From Karwoski CJ, Newman EA, Shimazaki H, et al: Light-evoked increases in extracellular K^+ in the plexiform layers of amphibian retinas. J Gen Physiol 86:189, 1985.)

(Fig. 24–5).[38, 50, 51, 76–80] Light-evoked $[K^+]_o$ increases occur in two regions within the retina. A brief $[K^+]_o$ increase occurs within the outer plexiform layer (OPL). This increase, termed the OPL K^+ increase,[80] is generated by K^+ release from depolarizing bipolar cells.[81] The increase is relatively small in amplitude (~0.1 mM) and occurs only at light onset; there is little, if any, increase at light offset.

A second light-evoked $[K^+]_o$ increase occurs within the inner plexiform layer (IPL). This $[K^+]_o$ increase, termed the IPL K^+ increase, is larger in magnitude (0.5 to 1.0 mM) and is more prolonged than is the outer plexiform layer increase. In addition, there is a prominent increase at light offset as well as at light onset. This increase is thought to be generated largely by depolarizing amacrine and ganglion cells,[79] although bipolar cells may also contribute.[81]

In dark-adapted retinae, light-evoked $[K^+]_o$ increases within the neural retina are accompanied by a $[K^+]_o$ decrease near the outer limiting membrane. This $[K^+]_o$ decrease is generated by the influx of K^+ into rod inner segments triggered by rod hyperpolarization.[82] The K^+ decrease spreads distally through the subretinal space to the RPE and proximally into the neural retina. The magnitude and duration of the K^+ decrease becomes larger as the duration of the light stimulus is increased. In the cat, $[K^+]_o$ within the subretinal space drops from a dark level of ~5 mM to 3 mM or less during prolonged illumination.[83]

CELL RESPONSES

The light-evoked responses of Müller cells are smaller and slower than are the responses of retinal neurons. Whereas photoreceptors and horizontal cells hyperpolarize 20 to 40 mV in response to a light flash, and ganglion cells generate a series of 90 mV action potentials, Müller cells rarely generate responses larger than 5 to 10 mV. In this respect, Müller cell responses are similar to those of other types of glial cells in the CNS.

The most prominent Müller cell response is a slow depolarization, a few millivolts in amplitude, with peaks at both the onset and offset of a stimulus (Fig. 24–6).[38, 79] This response is generated by the light-evoked $[K^+]_o$ increases within the retina, which shift the K^+ equilibrium potential in a depolarizing direction. The response is dominated by the inner plexiform layer $[K^+]_o$ increase, which is larger and more prolonged than is the increase in the outer plexiform layer. The time course of the Müller cell response directly parallels that of the light-evoked K^+ increase within the inner plexiform layer.[38] The Müller cell depolarization generates a substantial component of the ERG b-wave (see below and Chapter 25).

In the dark-adapted retina, sustained illumination evokes a second Müller cell response, a slow, prolonged cell hyperpolarization (see Fig. 24–6).[38, 50, 51] This response is generated by the $[K^+]_o$ decrease originating from the rod photoreceptors. The time course of the Müller cell hyperpolarization closely follows that of the $[K^+]_o$ decrease. This response contributes to the generation of the ERG c-wave (see below).

REGULATION OF $[K^+]_o$

As in other regions of the CNS, activity-dependent variations in $[K^+]_o$ within the retina must be regulated within close bounds in order to maintain normal neuronal function. The K^+ released by depolarizing neurons would lead to extremely large and rapid increases in $[K^+]_o$ if K^+ homeostatic mechanisms did not operate. In the retina, Müller cells are instrumental in regulating light-evoked $[K^+]_o$ variations.[84]

K^+ siphoning, a specialized form of K^+ spatial buffering,[85] is the principal mechanism by which Müller cells regulate $[K^+]_o$ (Fig. 24–7).[86] This homeostatic mechanism works in the following manner: Light-evoked $[K^+]_o$ increases within the retina generate an influx of K^+ into Müller cells. This passive influx depolarizes Müller cells and drives out an equal amount of K^+ from other cell regions. In species with avascular retinae, most K^+ channels are localized to the cell endfoot (see above) and passive K^+ efflux is concentrated in this region. This K^+, once it flows from the endfoot, will diffuse directly into the vitreous humor, which functions as a large K^+ sink, or reservoir.

The net effect of this K^+-siphoning mechanism is that K^+, released by retinal neurons, will be transferred by a current flow through Müller cells to the vitreous humor.[86, 87] Thus, $[K^+]_o$ within the retina is maintained

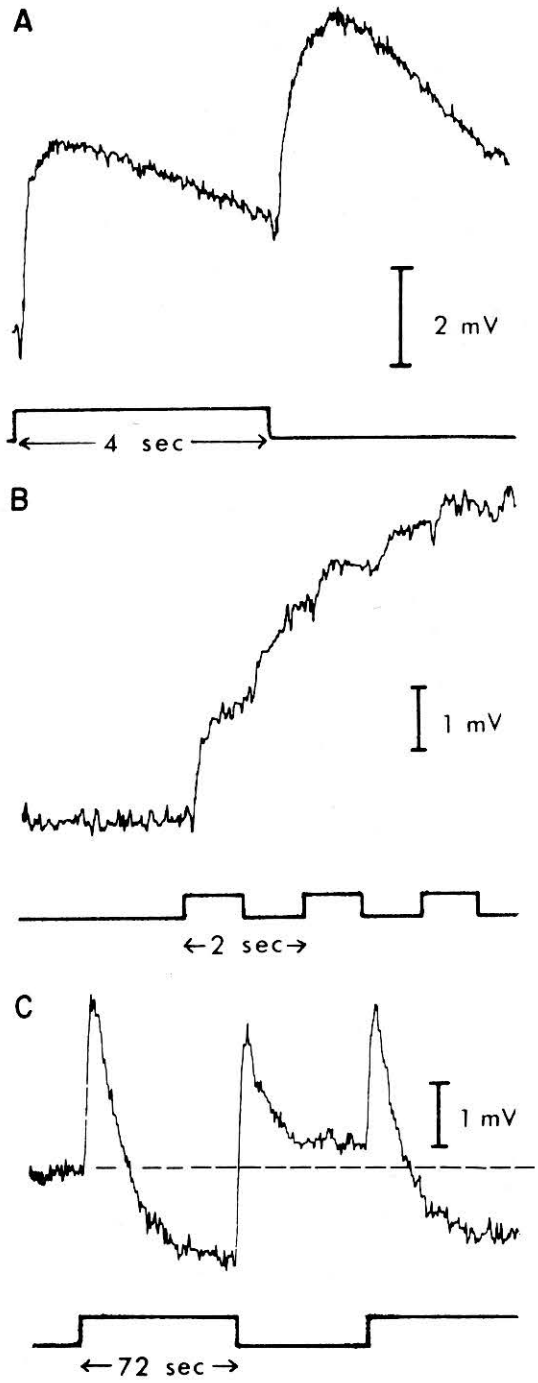

Figure 24–6. Light-evoked responses of Müller cells recorded from the mudpuppy (eyecup preparation). *A*, A 4-sec light flash (0.5-mm spot) evokes a slow cell depolarization with prominent on and off components. The depolarization generates the M-wave of the intraretinal ERG. Note the similarity between the cell response and the corresponding $[K^+]_o$ increase in the inner plexiform layer (see Fig. 24–5, IPL). *B*, Repetitive stimulation evokes progressively smaller Müller cell depolarizations that add together owing to the slow decay of the response. *C*, A prolonged light stimulus evokes an on depolarization followed by a sustained hyperpolarization. The hyperpolarization is generated by the $[K^+]_o$ decrease in the distal retina and generates the slow PIII potential. (From Karwoski CJ, Proenza LM: Relationship between Müller cell responses, a local transretinal potential, and potassium flux. J Neurophysiol 40:244, 1977.)

within closer limits than it would be without such a siphoning mechanism.

In the mammalian retina, Müller cell endfeet also have high K^+ conductance, and a similar K^+-siphoning mechanism may operate. In some mammalians, including the cat, however, K^+ conductance is largest at the distal (photoreceptor) end of Müller cells. In these species, K^+ may be siphoned from the distal end of Müller cells into the subretinal space. This K^+ may then be transferred to the choroidal circulation by a current flow across the RPE.[88]

K^+-siphoning currents flow through inward-rectifying K^+ channels in Müller cells. The voltage- and K^+-dependent properties of these channels function to enhance K^+ regulation by these cells. For example, when $[K^+]_o$ increases from 2.5 to 7.5 mM, Müller cell membrane conductance increases approximately threefold, thereby increasing the influx of K^+ into Müller cells and enhancing the transfer of K^+ to the vitreous humor via a K^+ current flow.

Direct experimental verification of K^+ siphoning has been obtained in the amphibian retina.[89] If light-evoked $[K^+]_o$ increases within the retina are buffered by K^+ siphoning, then efflux of K^+ from the Müller cell endfoot should lead to an increase in $[K^+]$ in the vitreous humor. Such light-evoked vitreal $[K^+]$ increases have been observed. When Müller cell K^+ channels are blocked, interrupting the K^+ siphoning current flow, the vitreal $[K^+]$ increase is nearly abolished.[89]

ELECTRORETINOGRAM GENERATION

Müller cells contribute to the generation of several components of the ERG, including the b-wave, the c-wave, the intraretinal M-wave, and the scotopic threshold response. A brief summary of Müller cell participation in ERG generation is given in this section. A more detailed description of the generation of b- and c-waves is given in Chapter 25.

b-Wave

The b-wave, or at least a substantial fraction of it, is generated by Müller cells in response to light-evoked $[K^+]_o$ increases within the retina (see Fig. 24–7). As described in the preceding section, a rise in $[K^+]_o$ generates a current flow through Müller cells. Current, in the form of a K^+ flux, enters Müller cells within the two plexiform layers and exits from the proximal end of the cell, near the inner limiting membrane.[90–93] The return current, flowing distally through extracellular space, generates a cornea-positive potential, the b-wave.

The b-wave reflects the light-evoked increase in $[K^+]_o$ in the outer plexiform layer more than it does the increase in the inner plexiform layer.[92, 94] This is because the K^+ increase in the outer plexiform layer is more transient and lies further from the Müller cell endfoot than does the inner plexiform layer increase. Current flowing from the cell endfoot must travel through a longer, and thus a higher-resistance, pathway to reach

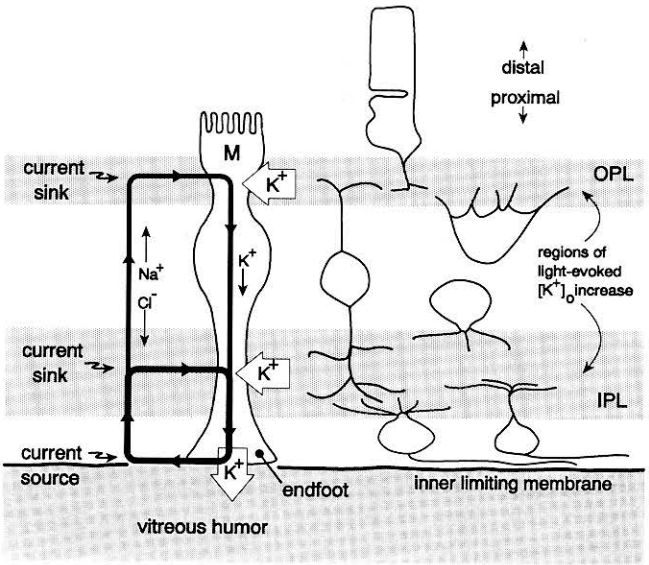

Figure 24–7. Müller cell regulation of $[K^+]_o$ and generation of the ERG b-wave in the amphibian retina. Depolarizing neurons within the retina release K^+, leading to light-evoked $[K^+]_o$ increases in the inner and outer plexiform layers. The $[K^+]_o$ increases result in influx of K^+ into Müller cells in the plexiform layers and in K^+ efflux from the cell endfoot *(open arrows)*. These K^+ fluxes establish a radially oriented current flow within the retina *(solid lines)*, which results in the transfer of K^+ from the retina to the vitreous humor. The current flow also generates a vitreous-positive potential, the ERG b-wave. M, Müller cell; OPL, outer plexiform layer; IPL, inner plexiform, layer. (Modified from Newman EA: Regulation of potassium levels by glial cells in the retina. Trends Neurosci 8:156, 1985.)

the outer plexiform layer. This leads to the generation of a larger voltage drop and a larger b-wave potential.[95] The transient $[K^+]_o$ increase within the outer plexiform layer is generated largely by the depolarizing bipolar cells.[81] Thus, the b-wave, in large part, is a reflection of depolarizing bipolar cell activity.

Although K^+ current flow through Müller cells accounts for a substantial portion of the b-wave, other Müller cell mechanisms may also contribute to the response. Light-evoked variations in extracellular glutamate concentration, the likely neurotransmitter of photoreceptors and bipolar cells, may lead to changes in currents generated by the Müller cell electrogenic glutamate uptake system and may contribute to b-wave generation.[63] Similarly, a GABA-activated Cl^- current could generate a transretinal potential.[74] Light-evoked changes in electrogenic HCO_3^- transport might also contribute to the generation of the ERG.

M-Wave

Müller cell current evoked by the inner plexiform layer $[K^+]_o$ increase also generates a retinal voltage, a potential termed the M-wave (M for Müller).[38, 79, 96] In contrast to the b-wave, the M-wave is observed only in intraretinal recordings (within the inner plexiform layer) and does not appear in the traditional corneal ERG.[97, 98] The M-wave is a slow negative potential that has prominent on and off peaks. It is spatially tuned, being maximally stimulated by small spot illumination.[38, 96] The response closely parallels the light-evoked $[K^+]_o$ increase in the inner plexiform layer in its threshold, dynamic range, and spatial tuning, indicating that the M-wave is generated by a K^+ current flow through Müller cells.[38, 79] The M-wave is abolished by Ba^{2+},[89] which blocks the K^+ channels of Müller cells.[42]

Scotopic Threshold Response

The scotopic threshold response (STR) is a second negative field potential generated by Müller cells in response to light-evoked increases in $[K^+]_o$ in the proximal retina.[98–100] It is a sustained negative response that decays without an off transient. It is distinguished from the M-wave in that it is rod driven and present at the dark-adapted threshold, and it is not spatially tuned.[99] The threshold and stimulus/response relation of the STR closely matches that of the light-evoked $[K^+]_o$ increase in the proximal retina, indicating that the response is generated by a K^+ flux through Müller cells. Like the M-wave, the STR is blocked by Ba^{2+}.[100, 101] The STR is a prominent component of the dark-adapted transretinal ERG and has been recorded in the monkey and humans as well as the cat.[98, 102, 103]

Slow PIII

Müller cells generate a cornea-negative transretinal voltage, the slow PIII potential, in response to the light-evoked K^+ decrease evoked by rod hyperpolarization.[82] This $[K^+]_o$ decrease, which originates at the rod inner segments, spreads into the neural retina and evokes an efflux of K^+ from the distal end of Müller cells. The resulting cell hyperpolarization elicits a K^+ influx from the proximal end of the cell. The return current flowing proximally through extracellular space generates the cornea-negative slow PIII potential.[90, 95, 104]

This mechanism of slow PIII generation has been confirmed in experiments on a number of species. The $[K^+]_o$ decrease, measured near the distal end of Müller cells, has the same time course as the Müller cell hyperpolarization and the slow PIII potential.[50, 51, 105] In addition, blocking Müller cell K^+ channels with Ba^{2+} abolishes both the Müller cell response and the slow PIII potential, but does not alter the $[K^+]_o$ decrease.[105, 106]

The slow PIII potential has a similar time course to the c-wave but is of opposite polarity; the c-wave is a cornea-positive potential, whereas the slow PIII is negative.[107] The positive component of the c-wave is generated by the RPE in response to the same rod-generated decrease in $[K^+]_o$ (see below). The corneal c-wave is actually the sum of the positive RPE potential and the negative Müller cell potential.

RETINAL PIGMENT EPITHELIUM

The retinal pigment epithelium is a single-layered cuboidal epithelium that lies between the retinal pho-

toreceptors and the choroid. The functions of the RPE are linked to those of the photoreceptors, with which they are closely associated. These functions are varied and have been likened to the functions of three different classes of cells: epithelial cells, glial cells, and macrophages.[7]

Like an epithelium, the RPE functions as a barrier between the choroidal circulation and the retina. In this capacity, it forms an important component of the blood-retinal barrier. Like other epithelia, it also transports ions, metabolites, and water between the retina and the choroid.

The RPE also has glial-like properties. The ion permeability of its apical membrane is dominated by a large K^+ conductance, and it generates voltage responses driven by variations in $[K^+]_O$. Like Müller cells, it is thought to regulate retinal ion levels. In addition, its processes cover a portion of the surface of a class of retinal neurons, the photoreceptors.

Finally, the RPE has macrophage-like properties; it functions to phagocytize and digest discarded portions of photoreceptor outer segments. Following retinal detachment, RPE cells can also differentiate into macrophages and phagocytize debris within the retina.

The RPE also serves a vital function in the visual cycle of retinoid metabolism and isomerization.

Structure

The RPE is a classic single-layered cuboidal epithelium (Fig. 24–8). Its basolateral membrane (which we will henceforth refer to as the basal membrane) lies adjacent to the choroidal capillaries. Its apical membrane, composed of microvillar processes, extends deep into the subretinal space as it interdigitates with photoreceptor outer segments.

The basal membrane of the RPE is bounded by a basal lamina that forms the most proximal layer (layer 5) of Bruch's membrane. The basal membrane is highly convoluted; its large surface area suggests that it subserves transport functions (see below).

Like other epithelia, adjacent RPE cells are joined by a complex series of junctions that separate the basal and apical surfaces of the cells. A continuous series of tight junctions encircle the cells, forming an effective diffusion barrier between the choroid and the retina.[108] Adjacent RPE cells are also joined by gap junctions that electrically couple the cells together.

The apical membrane of the RPE is composed of numerous microvillar extensions that project proximally into the subretinal space. The processes come in close contact with the photoreceptor outer segments. This association is particularly striking for cones (Fig. 24–9). In cat, cone outer segments are completely surrounded by multiple layers of sheetlike extensions of RPE processes.[109, 110] These processes appear to isolate cone outer segments from neighboring rod outer segments.

The cytoplasm of RPE cells have several prominent structures. The most striking are the melanin pigment granules that are distributed throughout the apical processes and the somata of RPE cells. The pigment granules serve to shield photoreceptors from scattered light and light passing through the sclera. (These pigment granules are absent from RPE cells in tapetal regions.) In lower vertebrates, pigment granules migrate up and down the apical processes as the adaptation state of the animal changes. In mammals, however, this motor response appears to be absent.

The second prominent cytoplasmic organelle is the lipofuscin granule, which represents the digested remains of outer segment discs that have been phagocytized by RPE cells. Lipofuscin is thought to be the final digestion product of this process.

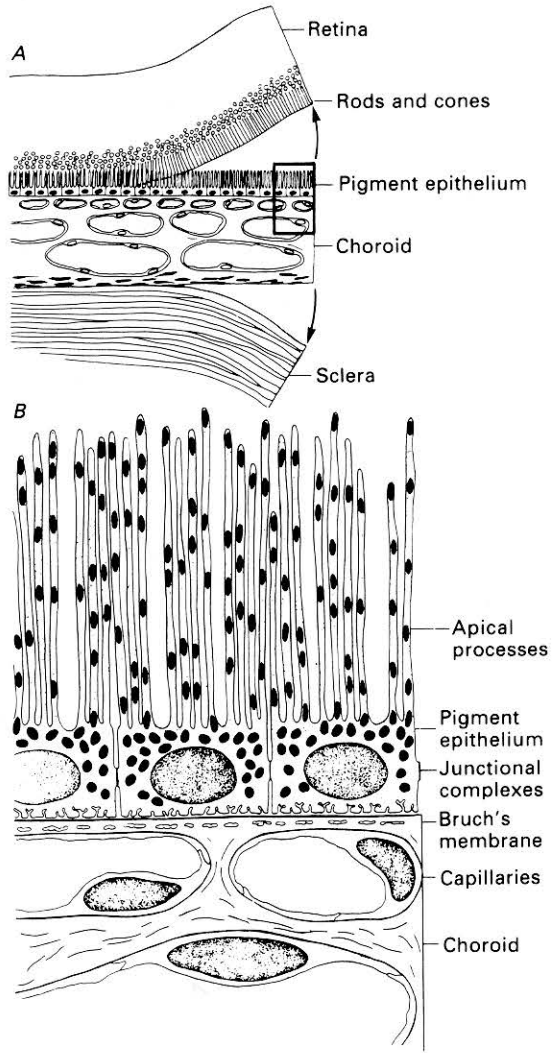

Figure 24–8. The bullfrog retina and retinal pigment epithelium (RPE). *A*, The relation between the RPE and neural retina. *B*, A detailed drawing of the RPE and choroid. The basic features of the mammalian RPE, including a convoluted basal membrane (adjacent to Bruch's membrane), junctions between cells, and apical processes, are similar to those illustrated here. Note that retinal orientation is opposite (vitreal side up) to that shown in Figs. 24–1, 24–3, 24–7, and 24–10. (From Hughes BA, Steinberg RH: Voltage-dependent currents in isolated cells of the frog retinal pigment epithelium. J Physiol 428:273, 1990.)

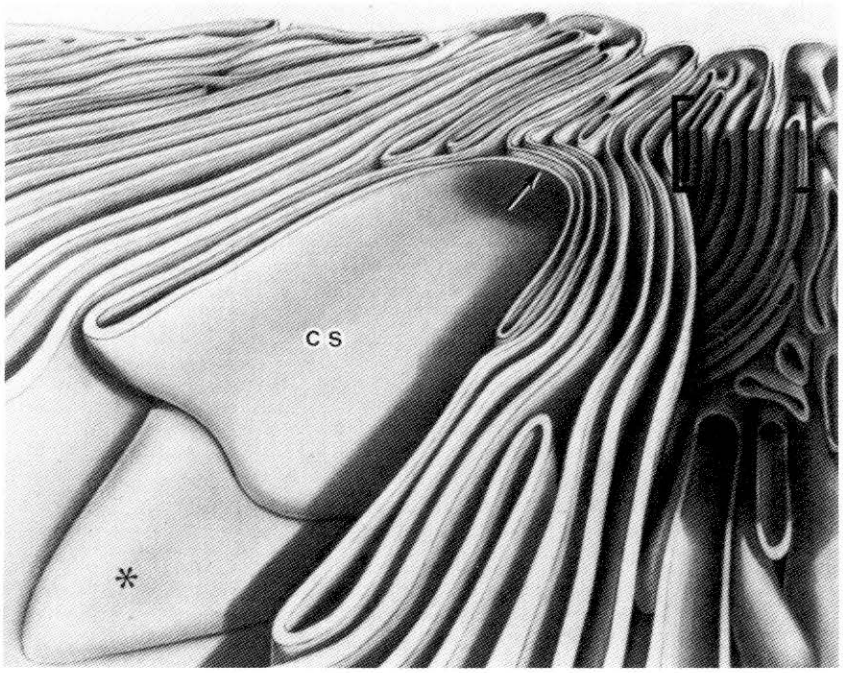

Figure 24–9. Diagram illustrating an RPE sheath of apical processes surrounding the outer segment of a cone (not shown). The view is from the retina looking distally (at an oblique angle) toward the RPE. The cone sheath (cs) is formed from a number of concentric lamellae of RPE apical processes that overlie the cone. One leaf-shaped RPE process is labeled with an asterisk. (From Fisher SK, Steinberg RH: Origin and organization of pigment epithelial apical projections to cones in cat retina. J Comp Neurol 206:131, 1982.)

Membrane Physiology

The membrane properties of the RPE have been studied using a number of techniques. Chamber measurements of closed-circuit currents and transepithelial voltages and fluxes have been used extensively in experiments on intact RPE tissue with choroid attached. In vivo and in vitro intracellular recordings of RPE responses have also been made. More recently, the properties of cultured and freshly isolated RPE cells have been studied with the patch-clamp technique. Most studies have utilized amphibian tissue, although experiments on mammals have been conducted in recent years, including some on freshly dissociated and cultured human tissue.

Early studies on amphibian tissue established that ions are actively transported across the RPE.[111–113] These studies demonstrated that Cl^- is transported from the apical to the basal side of the RPE and that Na^+ is transported in the opposite direction. In addition, a ouabain-sensitive Na^+/K^+-ATPase was shown to lie on the apical surface of RPE cells. More recently, several other transport systems have been identified on both the apical and basal membranes.

EPITHELIAL PROPERTIES

The epithelial nature of the RPE must be examined before the electrical and transport properties of these cells can be understood. The apical and basal membranes, along with the tight junctions joining the cells together, form a barrier to ion diffusion and electrical current flow.[114]

The apical and basal membranes of RPE cells have distinctly different properties. As detailed below, each surface has its own complement of ion channels and transporters. In addition, the two cell surfaces face different extracellular compartments having distinctly different resting and light-evoked ion compositions. Thus, the ion fluxes and membrane potentials that appear across the apical and basal membranes are different.

The membrane potential across the apical membrane of the RPE is termed V_{AP}.[9] This is the voltage measured by a microelectrode inside an RPE cell and referenced to fluid bordering the apical surface. Similarly, the membrane potential across the basal membrane is termed V_{BA}. The voltage across the entire RPE is termed the transepithelial potential, or TEP, and is defined by the relation

$$TEP = V_{BA} - V_{AP} \quad (2)$$

Thus, if V_{AP} is -80 mV and V_{BA} is -70 mV, TEP will be $+10$ mV (cornea positive).

Analysis of RPE responses is complicated by the fact that V_{AP} and V_{BA} are, to some extent, interdependent. A decrease in $[K^+]_O$ in the subretinal space, for instance, will cause a hyperpolarization of V_{AP}. This hyperpolarization will generate a current flowing inward across the basal membrane of the RPE and lead to a hyperpolarization of V_{BA} as well. The change in V_{BA}, however, is not as large as the change in V_{AP} and the initial hyperpolarization of V_{AP} results in a net increase in the TEP.

MEMBRANE CHANNELS AND TRANSPORTERS

An extensive array of ion channels and transport systems are found on the apical and basal membranes of the RPE. These are detailed in the following sections and are summarized in Figure 24–10.

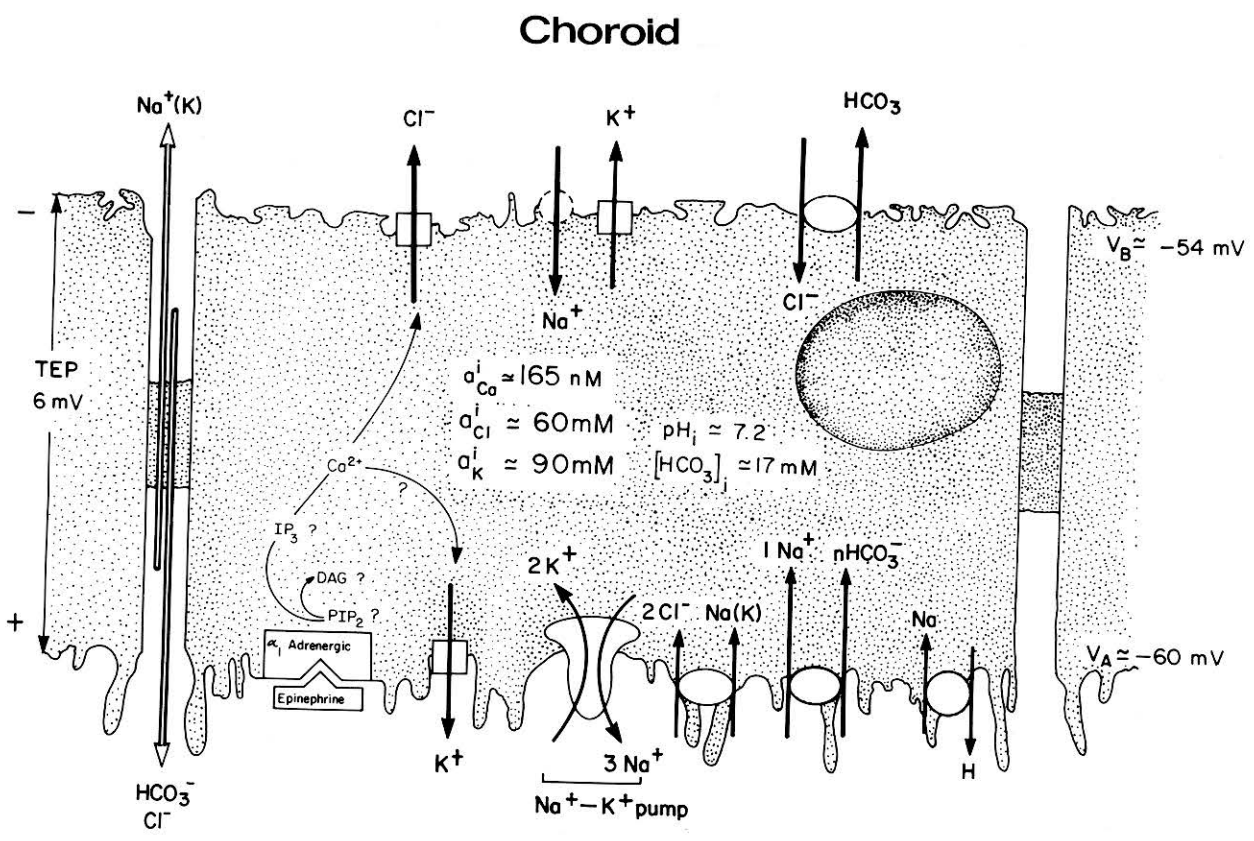

Figure 24–10. Summary of ion channels and transport systems present in bovine RPE cells. On the apical (lower) surface are, from left to right, an α_1-adrenergic receptor, a K^+ channel, a Na^+/K^+-ATPase, a $Na^+/K^+/Cl^-$ cotransporter, a Na^+/HCO_3^- cotransporter, and a Na^+/H^+ exchanger. On the basal (upper) surface are a Cl^- channel, a Na^+ channel, a K^+ channel, and a Cl^-/HCO_3^- exchanger. The dark bars between cells represent tight junctions. Arrows indicate the normal direction of ion fluxes. Voltages to the right are V_{AP} (V_A) and V_{BA} (V_B). (From Joseph DP, Miller SS: Apical and basal membrane ion transport mechanisms in bovine retinal pigment epithelium. J Physiol 435:439, 1991.)

Apical Membrane

K^+ Channel

The apical membrane of the RPE has a high K^+ conductance. This conductance is principally responsible for determining V_{AP}; increases and decreases in $[K^+]_O$ at the apical surface result in apical membrane depolarization and hyperpolarization, respectively. In contrast, variations in $[Cl^-]_O$ or $[Na^+]_O$ at the apical surface have little effect on V_{AP}, indicating that Na^+ and Cl^- channels are rare on this surface.[115]

The apical K^+ channels are blocked by Ba^{2+}. Addition of this divalent cation to the apical surface results in a substantial increase in the apical membrane resistance and in V_{AP} depolarization.[115] Whole-cell voltage-clamp recordings of dissociated amphibian RPE cells indicate that these K^+ channels have inward rectifying properties.[116] The channels are selectively permeable to K^+ but differ from the inward-rectifying K^+ channels of Müller cells and neurons in that their rectification is much less pronounced. Patch-clamp studies of freshly dissociated[117] and cultured[117, 118] human cells indicate the presence of several types of K^+ channels having different voltage-dependent properties and unitary conductances.

Na^+/K^+-ATPase

A Na^+/K^+-ATPase is localized to the apical membrane of RPE cells and is not present on the basal membrane. This localization is somewhat unique in that the Na^+/K^+ pump is found primarily on the basolateral surface in most other epithelia. (The choroid plexus of the brain is another exception to this rule.)

Like the Na^+/K^+ pumps of other cells, the RPE Na^+/K^+-ATPase is electrogenic and is inhibited by ouabain. Addition of ouabain to the apical (but not basal) surface of the RPE results in a rapid cell depolarization due to the cessation of the hyperpolarizing current generated by the pump. This is followed by a slower depolarization that reflects the rundown of the cell K^+ gradient. Ouabain also reduces K^+ influx into RPE cells[119] and the transport of Na^+ from basal to apical sides of the epithelium.[112]

The kinetic properties of the RPE pump have been characterized in some detail. Pump activity increases as external $[K^+]$ is raised from 0.2 to 5.0 mM.[120] In addition, the pump is inhibited by high levels of internal $[K^+]$.[121] The pump is temperature sensitive and is completely inhibited at low temperatures.[113]

$Na^+/K^+/Cl^-$ Cotransporter

Flux studies have demonstrated that there is a large Cl^- flux across RPE cells in an apical to basal direction.[112] This flux is believed to be driven by an electroneutral $Na^+/K^+/Cl^-$ cotransport system. There is strong evidence that such a cotransporter is present on the apical membrane of RPE cells. Furosemide and bumetanide, inhibitors of the $Na^+/K^+/Cl^-$ cotransporter, block transepithelial Cl^- transport in chick[122] and bovine retinae.[119] In cultured human RPE cells, Cl^- influx is dependent on the presence of external Na^+ and K^+ and is inhibited by bumetanide.[123] Cell volume regulation in amphibian RPE cells is dependent on the cotransporter; volume regulation is inhibited by bumetanide and by the removal of apical Na^+ and Cl^-.[124] The stoichiometry of the cotransporter in this system is $1Na^+:1K^+:2Cl^-$, accounting for its electroneutrality.[124]

The principal consequence of $Na^+/K^+/Cl^-$ cotransport in the RPE is that intracellular Cl^- concentration, $[Cl^-]_i$, rises to a substantially higher level than it would otherwise. This results in a Cl^- reversal potential in RPE cells that is far more depolarized than the cell resting potential.[115, 125]

The energy used to concentrate Cl^- inside RPE cells is supplied by the large Na^+ gradient across the apical membrane. This gradient powers the inward transport of Cl^- against its electrochemical gradient and results in high $[Cl^-]_i$. The K^+ that enters the cell along with Cl^- is removed by K^+ efflux through K^+ channels, largely from the apical surface[126]; this has been demonstrated by blocking apical K^+ channels with Ba^{2+}, which results in a net influx of K^+ in bovine RPE cells.[119] The influx of Na^+ via the cotransporter is balanced by its active extrusion via the Na^+/K^+-ATPase.

Na^+/HCO_3^- Cotransport

An electrogenic Na^+/HCO_3^- cotransport system is also present on the apical membrane of RPE cells. A decrease in either Na^+ or HCO_3^- at the apical surface results in a depolarization of V_{AP}, a reduction in $[Na^+]_i$, and cell acidification.[127, 128] These responses are generated by a coupled flux of HCO_3^-, Na^+, and a negative charge via a Na^+/HCO_3^- cotransporter. Cotransporter fluxes are blocked by the disulfonic stilbenes DIDS and SITS. The stoichiometry of the cotransporter in frog is $\sim 2HCO_3^-:1Na^+$.[127]

In the frog, the reversal potential of the Na^+/HCO_3^- cotransporter (~ -114 mV) is more negative than V_{AP}. Thus, the cotransporter supports an inwardly directed flux of Na^+ and HCO_3^- across the apical membrane. This influx of HCO_3^- maintains internal $[HCO_3^-]$ higher than it would be if it were at its electrochemical equilibrium. The cotransporter is also instrumental in regulating pH following an acid load. In the frog, 80 to 90 percent of pH recovery from an acid load is mediated by the Na^+/HCO_3^- cotransport system.[129] The RPE cotransporter has, to date, been characterized only in amphibian cells.

Na^+/H^+ Antiporter

An Na^+/H^+ antiporter constitutes a second acid/base transport system on the apical surface of RPE cells. In frog, this antiporter plays a minor role in pH recovery following an acid load. In the absence of HCO_3^- at the apical surface, amiloride, a Na^+/H^+ antiport blocker, inhibits pH recovery attributable to the antiport system.[129]

Basal Membrane

K^+ Channel

Like the apical membrane, the basal membrane of the RPE has a high conductance to K^+. Increasing basal $[K^+]_o$ results in a depolarization of V_{BA},[115, 130] as does addition of the K^+ channel blocker Ba^{2+}.[115] Ba^{2+} also blocks the efflux of K^+ from the basal surface of RPE cells.[88]

Cl^- Channel

In contrast to the apical membrane, the basal membrane of the RPE has a substantial conductance to Cl^-. In the toad, reduction of basal $[Cl^-]_o$ results in depolarization of V_{BA}, a decrease in $[Cl^-]_i$, and an increase in the resistance of the basal membrane.[130] These responses to lowered $[Cl^-]_o$ are blocked by DIDS, an agent that blocks anion channels. These observations are consistent with the presence of a large Cl^- conductance on the basal membrane. This conductance contributes significantly to the determination of V_{BA}. In the toad, ~45% of the basal membrane conductance is estimated to be due to the Cl^- conductance.[130]

Similar observations have been made in chick[125] and bovine retinae.[115] Basal DIDS application in these species results in a hyperpolarization of V_{BA}, indicating that the basal Cl^- equilibrium potential, which is more positive than the K^+ potential, contributes to V_{BA}. The basal Cl^- conductance ensures that V_{BA} is more depolarized than is V_{AP} and that TEP is positive.

Cl^-/HCO_3^- Exchanger

An electroneutral Cl^-/HCO_3^- anion exchanger is also believed to be present on the basal membrane of the RPE. Definitive evidence for this antiport system is lacking, but the exchanger is thought to be responsible for the efflux of HCO_3^- from the RPE basal membrane. Variations in basal HCO_3^- have no effect on V_{BA},[131] indicating that HCO_3^- transport is electroneutral. Reduction of basal $[HCO_3^-]_o$ leads to an increase in $[Cl^-]_i$, consistent with a Cl^-/HCO_3^- exchange mechanism.[132]

FLUID TRANSPORT

One of the principal functions of the retinal pigment epithelium is the transport of fluid from the subretinal space to the choroid.[133] This fluid transport is thought to play an important role in adhesion of the neural retina to the RPE.

As in other epithelia, fluid transport is accomplished by the transfer of ions from one side of the epithelium to the other. The osmotic imbalance created by this ion transport drives the subsequent movement of water. In the RPE, water movement is powered principally by the transport of Cl^- and HCO_3^- from the apical to basal surface.

Cl^- Flux

Flux studies have demonstrated that there is a net transport of Cl^- from the apical to basal membrane of the RPE.[112] This transport occurs principally via the $Na^+/K^+/Cl^-$ cotransporter on the apical membrane and Cl^- channels on the basal membrane.

The driving force for Cl^- transport is supplied by the Na^+ gradient across the apical membrane. The inward Na^+ gradient powers the coupled influx of Na^+, K^+, and Cl^- through the bumetanide-sensitive $Na^+/K^+/Cl^-$ cotransporter. This influx results in a $[Cl^-]_i$ that is substantially larger than its equilibrium concentration. In the bovine RPE, for instance, $[Cl^-]_i$ is approximately fivefold larger than it would be if it were at its electrochemical equilibrium.[115] A similar situation has been found in the toad[130] and chick.[125]

The large $[Cl^-]_i$ results in a Cl^- equilibrium potential more positive than V_{AP} and V_{BA}. This outwardly directed electrochemical potential powers an efflux of Cl^- through the Cl^- channels of the basal membrane. The net effect of these processes is to transport Cl^- from the subretinal space to the choroid.

HCO_3^- Flux

HCO_3^- transport across the RPE also occurs in the apical to basal direction and is believed to contribute to fluid transport from the subretinal space. In the frog, for instance, fluid transport is reduced by 70% when HCO_3^- is removed from apical and basal solutions.[134] HCO_3^- transport is thought to occur via the electrogenic Na^+/HCO_3^- cotransporter on the apical membrane and the anion exchanger on the basal membrane.

As is the case for Cl^- transport, the principal driving force for HCO_3^- flux is the inward Na^+ gradient across the apical membrane. This gradient drives the coupled influx of Na^+ and HCO_3^- via the apical Na^+/HCO_3^- cotransporter and results in an accumulation of HCO_3^- within the RPE. This HCO_3^-, in turn, is transported out of the cell via the electroneutral Cl^-/HCO_3^- exchanger on the basal membrane. The effect of these processes is to transport HCO_3^- from the subretinal space to the choroid.

NEUROTRANSMITTERS

Neurotransmitters have a profound influence on RPE function. Transmitters and second-messenger systems have been shown to modulate RPE membrane voltage and resistance, ion and fluid transport, and, in lower vertebrates, pigment granule aggregation and dispersion. The effects of neurotransmitters are complex, and in some cases, they differ depending on the species and transmitter concentration used. Neurotransmitter modulation of the RPE is of great interest as it constitutes an important path for communication between the neural retina and the epithelium.

Epinephrine

In the bovine retina, epinephrine increases the TEP by depolarizing V_{BA}.[135] This depolarization results from an increase in basal Cl^- conductance and is blocked by basal DIDS or apical bumetanide.[136] The response is mediated by an α_1-adrenergic receptor on the apical membrane and results in an enhancement of fluid transport across the RPE.[137]

Epinephrine has a similar effect on the isolated, perfused cat eye, where it increases the standing potential, most likely by depolarizing V_{BA}[138] and increasing the TEP. Epinephrine decreases the light peak and increases the c-wave in the cat, consistent with an increase in basal membrane conductance (see below).

Epinephrine also causes an increase in the TEP in sheets of cultured human RPE cells, presumably by depolarizing V_{BA}.[139] This response is mediated by a β-adrenergic receptor and is coupled to a cyclic adenosine monophosphate (cAMP) second-messenger system. In the rabbit, in contrast, epinephrine decreases TEP. This response is believed to be mediated by an α_1 receptor.[140]

Dopamine

The catecholaminergic neurotransmitter dopamine is of special interest when considering RPE function because it is a transmitter utilized by retinal neurons. Light-evoked variations in retinal dopamine levels will be sensed by the RPE and may modulate its function. In lower vertebrates, dopamine regulates pigment migration in RPE cells, causing a dispersion of granules into the apical processes.[141]

The effects of dopamine in the RPE are similar to those of epinephrine. In bovine RPE cells, dopamine application results in a depolarization of V_{BA} and a decrease in basal membrane resistance.[135] This response is presumably mediated by an increase in basal Cl^- conductance. Dopamine is less effective than epinephrine in this system. In the isolated cat eye, dopamine generates an increase in the standing potential, indicating a presumed increase in the TEP and a depolarization of V_{BA}.[138]

The effect of dopamine in chick RPE cells is somewhat more complex. At most concentrations tested, dopamine causes a biphasic response, a hyperpolarization of V_{BA}, and an increase in basal membrane resistance followed by a depolarization of V_{BA} and a decrease in membrane resistance.[142] The dopamine effects are blocked by basal DIDS, suggesting that the transmitter is modulating basal Cl^- conductance, perhaps via a second-messenger system.

Melatonin

Melatonin, an indolamine hormone synthesized by retinal neurons, also modulates basal membrane resistance. In the chick, melatonin reduces the TEP, a response generated by hyperpolarization of V_{BA} and an increase in basal resistance.[143] In the cat, on the other hand, melatonin increases the TEP, albeit weakly.[138]

Cyclic AMP

Cellular responses to epinephrine (α_2 and β receptors), dopamine (D1 and D2 receptors), and melatonin

are mediated by the cAMP second-messenger system. The effect of cAMP on RPE cells is therefore of great interest. Numerous studies have demonstrated that cAMP has striking and complex effects on the retinal pigment epithelium.

In the frog, cAMP causes a large and rapid decrease in fluid transport from the apical to basal surface of the RPE.[134, 144] This effect may be due to cAMP modulation of basal Cl^- conductance. Cyclic AMP, phosphodiesterase inhibitors, and forskolin all cause an increase in the TEP, a response generated by V_{BA} depolarization.[145] The depolarization is associated with an increase in the conductance of the basal membrane, presumably due to modulation of Cl^- channels. This conductance increase may be transient, however, changing to a conductance decrease at longer times.[146] Cyclic AMP has the secondary effect in the frog of increasing Na^+/K^+-ATPase activity on the apical membrane, most likely because of increased Na^+ influx via the $Na^+/K^+/Cl^-$ cotransporter.[146]

In the isolated cat eye, cAMP has an effect similar to that of the catecholaminergic transmitters; it increases the TEP, presumably by increasing basal membrane conductance to Cl^-.[138] In the chick, on the other hand, cAMP appears to have the opposite effect. Addition of cAMP and/or the phosphdiesterase inhibitor IBMX results in a decrease in the TEP, a response generated by a hyperpolarization of V_{BA}.[147] Basal hyperpolarization is accompanied by an increase in basal membrane resistance, most likely arising from a reduction in Cl^- conductance. This response parallels the effect of low concentrations of dopamine in the chick, which also produces an increase in basal membrane resistance.[142]

Light-Evoked Responses

$[K^+]_o$ DECREASE

Several components of the DC-recorded ERG and all of the components of the electro-oculogram (EOG) are generated by the retinal pigment epithelium. These light-evoked responses include the c-wave, the fast oscillation, and the light peak. In addition, the standing potential of the EOG is generated principally by the RPE.

The c-wave and fast oscillation of the RPE reflect variations in $[K^+]_o$ within the subretinal space. K^+-selective microelectrode recordings demonstrate that a slow decrease in $[K^+]_o$ in the subretinal space occurs at light onset (Fig. 24–11). $[K^+]_o$ drops from a dark level of ~5 to 2 mM or less in the light.[76, 83] The action spectrum of the decrease reveals that it is generated by rod photoreceptors.[76] The decrease results from rod hyperpolarization, which reduces the passive efflux of K^+ from rod inner segments.[82] The continued action of the Na^+/K^+-ATPase in rod inner segments leads to a net influx of K^+ and to a decrease in $[K^+]_o$.

CELL HYPERPOLARIZATION AND $[K^+]_o$ REGULATION

The $[K^+]_o$ decrease in the subretinal space generates the principal light-evoked response of the RPE, a slow cell hyperpolarization at light onset. In mammals, the response to a brief light flash peaks after 2 to 4 sec. Its time course is even slower in lower vertebrates. The slow time course of this response, which differs from the rapid responses of retinal neurons, arises because of the slow variations in $[K^+]_o$ within the subretinal space.

The RPE hyperpolarization is generated by the change in the K^+ equilibrium potential at the apical membrane. A drop in $[K^+]_o$ in the subretinal space hyperpolarizes V_{AP} and results in a cell hyperpolarization (Fig. 24–12).[148, 149] (The drop in apical $[K^+]_o$ also reduces Na^+/K^+-ATPase activity [see above] and thus depolarizes V_{AP} somewhat. This depolarization is substantially smaller than the hyperpolarization due to the change in the K^+ equilibrium potential, however.)

The time course of the $[K^+]_o$ decrease closely matches the time course of RPE hyperpolarization[76, 83] and is thought to be exclusively responsible for the RPE response.[150] Lowering apical $[K^+]_o$ experimentally generates the expected hyperpolarization of V_{AP}.

RPE hyperpolarization results in an increased driving force for K^+ entry from the choroid through the basal membrane. K^+-selective microelectrode measurements demonstrate that a decrease in $[K^+]_o$ at the apical

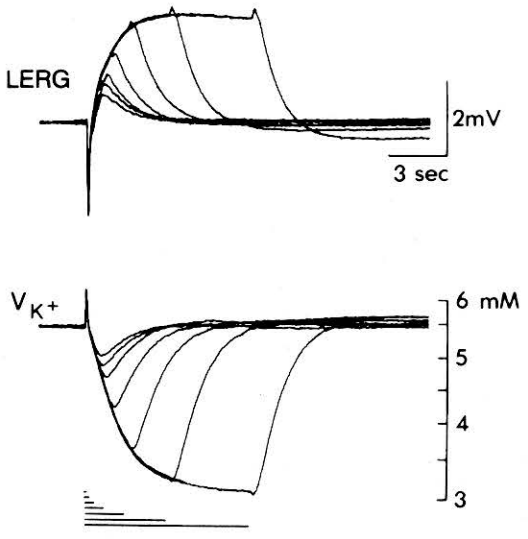

Figure 24–11. Light-evoked $[K^+]_o$ decrease and intraretinal ERG recorded simultaneously from the subretinal space of the cat retina (intact eye preparation). $[K^+]_o$ in the subretinal space (V_{K^+}) falls slowly from a resting level of 5.5 mM to nearly 3 mM when a light stimulus is turned on. The positive component of the intraretinal ERG (LERG), which is the intraretinal equivalent of the c-wave, displays a nearly identical time course as the $[K^+]_o$ decrease. The initial, negative component of the LERG is the intraretinal b-wave. Superimposed waveforms show responses to seven different stimulus durations. (From Steinberg RH, Oakley B II, Neimeyer G: Light-evoked changes in $[K^+]_o$ in retina of intact cat eye. J Neurophysiol 44:897, 1980.)

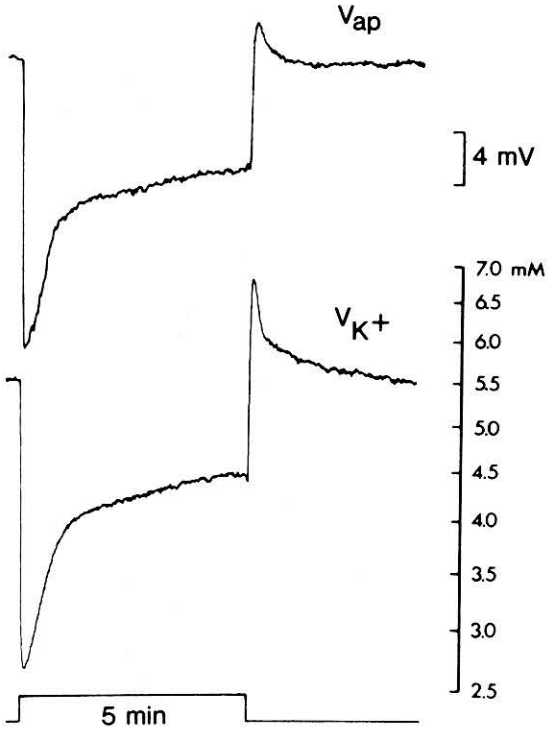

Figure 24–12. Light-evoked $[K^+]_o$ decrease and RPE membrane potential recorded from the cat retina (intact eye preparation). The $[K^+]_o$ decrease (V_{K^+}), recorded from the subretinal space, is shown at a slower time scale than in Figure 24–11 and displays a partial recovery from its maximal decrease. The RPE membrane hyperpolarization (V_{ap}), recorded across the apical membrane, shows a nearly identical time course, indicating that the hyperpolarization is generated by the $[K^+]_o$ decrease. (From Linsenmeier RA, Steinberg RH: Delayed basal hyperpolarization of cat retinal pigment epithelium and its relation to the fast oscillation of the DC electroretinogram. J Gen Physiol 83:215, 1984.)

surface, produced either by light stimulation or by direct perfusion of the apical membrane, results in a decrease in $[K^+]_o$ at the basal membrane.[88] This basal decrease indicates that a basal to apical flux of K^+ is evoked when $[K^+]_o$ within the subretinal space drops.[126] This flux partially offsets the light-evoked $[K^+]_o$ decrease at the apical surface, helping to maintain $[K^+]_o$ levels in the subretinal space. This K^+ regulation mechanism[88] is a form of spatial buffering, a process that also occurs in Müller cells and other CNS glial cells.[85, 86, 151]

ELECTRORETINOGRAM GENERATION

c-Wave

The c-wave of the ERG (Fig. 24–13) is generated by the summation of a cornea-positive RPE potential and a cornea-negative Müller cell potential, the slow PIII (see above). The RPE potential is larger than is the Müller cell potential and a cornea-positive response results. The RPE component of the response is generated by the RPE hyperpolarization evoked by the $[K^+]_o$ decrease in the subretinal space.[148] The $[K^+]_o$ decrease lowers the K^+ equilibrium potential at the apical membrane and hyperpolarizes V_{AP}. This hyperpolarization results in an increase in TEP, which is recorded as a cornea-positive potential. The time course of this potential is almost identical to that of the original $[K^+]_o$ decrease in the subretinal space[150] (see Fig. 24–12).

Hyperpolarization of V_{AP} results in a passive hyperpolarization of V_{BA} as well. The V_{BA} hyperpolarization is smaller than is the V_{AP} hyperpolarization, however, and a net positive TEP results.[150] The magnitude of the V_{BA} hyperpolarization depends on the resistance of the basal membrane. Thus, a decrease in basal membrane resistance, such as occurs during the light peak (see below) results in a smaller V_{BA} hyperpolarization and in a larger c-wave.[152] Similarly, an increase in basal membrane resistance, which occurs during the fast oscillation (see below), results in a larger V_{BA} hyperpolarization and in a smaller c-wave.

Fast Oscillation

The fast oscillation trough is a corneal-negative dip in the DC ERG that follows the c-wave. Contrary to that implied by its name, the fast oscillation is a very slow response, beginning several seconds after the onset of illumination, peaking at ~20 sec, and decaying over a period of a minute. (The response is more rapid than the light peak, hence the name *fast* oscillation.) The response is generated by the RPE and arises from a delayed hyperpolarization of the basal membrane and an associated increase in basal membrane resistance.[153, 154]

The delayed V_{BA} hyperpolarization of the fast oscillation is coupled to the light-evoked apical $[K^+]_o$ decrease and to V_{AP} hyperpolarization.[115] Experimental reduction of apical $[K^+]_o$ and the resulting V_{AP} hyperpolarization in the gecko[155] and the bovine retinae[115] is followed by a delayed V_{BA} hyperpolarization.

The delayed V_{BA} hyperpolarization is related to Cl^- transport and may be mediated by a reduction in $[Cl^-]_i$.

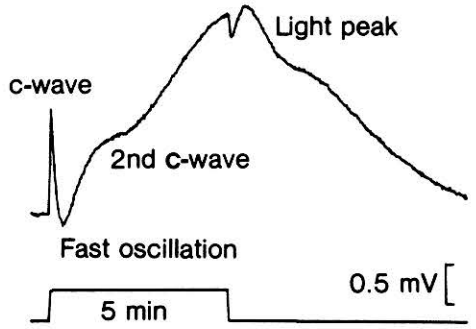

Figure 24–13. The DC ERG recorded from the vitreous of the intact cat eye. The c-wave (initial positive transient), the fast oscillation (the negative dip that follows) and the light peak (the second, slow positive peak) are seen. The small trough at the peak of the light peak is an off response. The a- and b-waves are too rapid to be seen in this ERG record. (From Linsenmeier RA, Steinberg RH: Delayed basal hyperpolarization of cat retinal pigment epithelium and its relation to the fast oscillation of the DC electroretinogram. J Gen Physiol 83:213, 1984.)

V_{AP} hyperpolarization, generated by the light-evoked apical $[K^+]_O$ decrease, leads to an enhanced efflux of Cl^- through the basal membrane Cl^- channels. The resulting reduction in $[Cl^-]_i$[115] makes the Cl^- reversal potential at the basal membrane more negative. As a result, V_{BA} hyperpolarizes and the TEP is reduced. The increase in basal membrane resistance, which accompanies V_{BA} hyperpolarization, is thought to result from a reduction in the number of anion charge carriers within the cell.

Evidence supporting this mechanism of fast oscillation generation includes the following: (1) a decrease in $[Cl^-]_i$ is associated with the delayed V_{BA} hyperpolarization[115]; (2) the fast oscillation is reduced by basal DIDS, which blocks Cl^- channels on the basal membrane[115, 156]; (3) voltage-dependent conductances on the basal membrane play little or no role in the increase in basal membrane resistance and V_{BA} hyperpolarization[157]; and (4) patients with cystic fibrosis, a genetic disorder affecting Cl^- transport in epithelia, have reduced fast oscillation potentials.[158]

Light Peak

The light peak is a cornea-positive response generated by the RPE. It has a very slow time course, trailing the fast oscillation and peaking at ~5 min after the onset of illumination. The electrical mechanism by which this response is generated is complementary to that of the fast oscillation; the light peak arises from a depolarization of V_{BA} and is associated with a decrease in the resistance of the basal membrane.[159] The fast oscillation, in contrast, is generated by a hyperpolarization of V_{BA} and an increase in basal membrane resistance. The depolarization of V_{BA} is believed to be generated from an increase in basal Cl^- conductance. The light peak is abolished when basal Cl^- channels are blocked with DIDS.[156]

Unlike the c-wave and the fast oscillation, the light peak is not triggered by the light-evoked reduction in subretinal $[K^+]_O$. Rather, an as yet unidentified "light peak substance" is thought to modulate basal Cl^- conductance, perhaps via a second-messenger system. Systemic or intravitreal application of dopamine in the chicken increases the standing potential voltage,[160] whereas haloperidol block of dopamine receptors decreases the standing potential and strongly reduces or abolishes the light peak.[161] Dopamine and melatonin, when applied to the chick-retinal-RPE preparation, reduce or abolish the light peak, presumably by modulating basal Cl^- conductance.[142, 143] Similarly, epinephrine is believed to increase basal Cl^- conductance in a variety of tissues.[135, 138, 139] However, these transmitters may be producing their effect on the basal membrane in a nonspecific fashion and may not be the true "light peak substance."

Transepithelial Potential and the Standing Potential

The apical membrane of the RPE, dominated by its large K^+ conductance, is more hyperpolarized than is the basal membrane, which is permeable to both K^+ and Cl^-. Thus, the TEP is positive and generates a positive potential at the cornea when referenced to a distant ground. This potential is recorded as the standing potential of the EOG.

Variations in the TEP of the retinal pigment epithelium, such as occur with depolarization or hyperpolarization of V_{BA}, are recorded as changes in the standing potential. For instance, mild hypoxia[162] and application of sodium azide[163] in the cat depolarize V_{BA} and result in an increase in the standing potential. Mild hypoxia in the human also leads to an increase in the standing potential,[164] presumably by a similar effect on V_{BA}.

Visual Cycle

One of the essential functions of the RPE is its participation in the visual cycle of retinoid metabolism and isomerization. The role of the RPE in the visual cycle is discussed in detail in Chapter 18 and will only be summarized briefly here. The reader is also referred to other recent reviews of the subject.[6, 10]

The retinal pigment epithelium plays a vital role in the visual cycle. Its functions include (1) uptake of all-*trans*-retinol (vitamin A) from the blood, (2) storage of retinoids within the RPE, (3) isomerization of retinoids to the 11-*cis* form, and (4) transfer of retinoids to the photoreceptors.

Retinoids are highly hydrophobic and are almost insoluble in water. They are solubilized in the blood and within cells (and protected from oxidation) by being bound to retinoid-binding proteins. In the blood, all-*trans*-retinol is bound to RBP (retinoid-binding protein) and serves as the source of retinoids in the retina. All-*trans*-retinol is transferred from the choroidal circulation, across the basal membrane of the RPE, and bound within the epithelial cells by CRBP.

All-*trans*-retinol enters directly into the visual cycle at this point. A membrane-bound retinyl ester synthetase esterifies all-*trans*-retinol to all-*trans*-retinyl ester. Retinyl ester, in turn, is converted to 11-*cis*-retinol by a retinoid isomerase. The retinyl ester synthetase and the retinoid isomerase are believed to be complexed together within the RPE. The energy required to isomerize the retinoid from the all-*trans* form to the 11-*cis* form is supplied by the hydrolysis of the retinyl ester in this coupled reaction. The 11-*cis*-retinol, now bound to CRalBP is oxidized to 11-*cis*-retinal. (This reaction can take place in amphibian photoreceptors. In mammals, however, the oxidation of retinol is believed to occur solely within the RPE.)

11-*cis*-Retinal produced by the RPE is transferred across the subretinal space, bound to interphotoreceptor retinoid-binding protein (IRPB). When it reaches the photoreceptor outer segments, it combines with bleached opsins and forms regenerated photopigments.

The visual cycle is completed as the photopigments in the rods and cones are bleached. Bleaching causes a photoisomerization of the chromophore to all-*trans*-retinal, which is released from the opsin and reduced to all-*trans*-retinol within the outer segments. All-*trans*-

retinol is then transferred back to the RPE bound to IRBP within the subretinal space. Within the RPE, it is bound to CRBP and once again is reisomerized to the 11-*cis* form.

Phagocytosis

The RPE plays an essential role in the renewal of photoreceptors by phagocytosing and digesting the shed distal ends of photoreceptor outer segments. This function of the RPE is reviewed in detail elsewhere and will only be discussed briefly here. The reader is also referred to a review of the subject.[8]

Both rods and cones shed the distal ends of their outer segments in a rhythmic pattern entrained to the light-dark cycle.[165–167] The shed portion of the outer segment is replaced with newly synthesized discs that are added to the base of the outer segment. This renewal process is dependent on the efficient removal of the shed portions of the outer segment. The job falls to the retinal pigment epithelium, which phagocytoses the shed debris. The outer segment debris is enveloped by large actin-containing pseudopodia of the RPE apical processes. The shed outer segments are internalized and digested in phagosomes within the RPE. The phagosomes are displaced toward the basal surface of the RPE as digestion proceeds and as their contents become deformed and compacted. Undigested portions of outer segment material remain within RPE cells and accumulate to form lipfuscin granules, which collect as RPE cells age.[168]

Retinal pigment epithelium phagocytosis illustrates the macrophage-like properties of these cells. This capability is actually expressed under pathologic conditions. When the retina detaches from the underlying RPE, RPE cells proliferate and differentiate into motile cells that resemble macrophages in morphology and behavior.[169, 170] These differentiated cells migrate through the retina and can undergo massive proliferation, forming epiretinal membranes on the retinal surface.[170] Interestingly, Müller cells also express macrophage-like properties and can phagocytose foreign particles introduced into the retina.[171]

Trophic Support of the Retina

Evidence suggests that the RPE produces substances that may be required for the normal growth and maintenance of photoreceptors.[172] Recent work with the retinal dystrophic RCS rat mutant suggests one possible function of RPE cells in photoreceptor maintenance.

The photoreceptors of rats carrying the RCS mutant degenerate within the first few months of life. The mutation is expressed in RPE cells rather than in photoreceptors; in chimeric animals that have adjacent regions of normal and mutant tissue, photoreceptor degeneration occurs only in those regions directly opposed to mutant RPE tissue.[173] Photoreceptor degeneration can be prevented in mutant animals by transplantation of normal RPE cells.[174, 175] In both the chimeric animals and in the transplant experiments, the region of photoreceptor rescue extended somewhat beyond the region of normal RPE cells, suggesting that a diffusible substance produced by the RPE was preventing photoreceptor degeneration. Degeneration can also be prevented by injection of basic fibroblast growth factor (bFGF) into the eyes of RCS animals.[176] The RPE cells express the bFGF gene and synthesize the peptide.[177, 178] Together, these experiments suggest that RPE cells play an important role in the maintenance of normal photoreceptor function, perhaps by releasing trophic substances such as bFGF.

SUMMARY

Müller cells and retinal pigment epithelium cells are the two principal nonneuronal cells intrinsic to the retina. They share a neural epithelial origin and retain many epithelial features. They both play essential roles in maintaining retinal function, with Müller cells supporting the neural retina and the RPE supporting the photoreceptor outer segments.

Müller cells and RPE cells are both principally permeable to K^+ and generate light-evoked potentials in response to variation in $[K^+]_o$. These potentials generate transretinal voltages that are recorded as components of the ERG and the EOG. Both Müller cells and RPE cells have specific ion channels and transport systems that are localized to particular cell regions. In the case of the RPE, these channels and transporters are instrumental in generating transepithelial ion fluxes and fluid transport. Similar transport processes may occur in Müller cells.

Regulation of the extracellular environment is an important function of both Müller cells and RPE cells. Müller cells regulate extracellular ion levels throughout much of the neural retina and play an important role in terminating synaptic transmission by active uptake of neurotransmitters. The RPE cells regulate ion levels in the region of the photoreceptor outer segments and supply the photoreceptors with the isomerized retinoids essential for phototransduction.

REFERENCES

1. Rodieck RW: The Vertebrate Retina: Principles of Structure and Function. San Francisco, WH Freeman, 1973, pp 1–1044.
2. Young RW: The life history of retinal cells. Trans Am Ophthalmol Soc 81:193, 1983.
3. Ripps H, Witkovsky P: Neuron-glia interaction in the brain and retina. Prog Retinal Res 4:181, 1985.
4. Newman EA. The Müller cell. *In* Federoff S, Vernadakis A (eds): Astrocytes, vol 1. Orlando, FL, Academic Press, 1986, pp 149–171.
5. Newman EA: Electrophysiology of retinal glial cells. Prog Retinal Res 8:153, 1988.
6. Bok D: Processing and transport of retinoids by the retinal pigment epithelium. Eye 4:326, 1990.
7. Steinberg RH: Interactions between the retinal pigment epithelium and the neural retina. Doc Ophthalmol 60:327, 1985.
8. Bok D: Retinal photoreceptor-pigment epithelium interactions. Invest Ophthalmol Vis Sci 26:1659, 1985.
9. Steinberg RH, Linsenmeier RA, Griff ER: Retinal pigment epithelial cell contributions to the electroretinogram and electrooculogram. Prog Retinal Res 4:33, 1985.

10. Saari JC: Enzymes and proteins of the mammalian visual cycle. Prog Retinal Res 9:363, 1990.
11. Newman EA: Sodium-bicarbonate cotransport in retinal Müller (glial) cells of the salamander. J Neurosci 11:3972, 1991.
12. Bunt-Milam AH, Saari JC: Immunocytochemical localization of two retinoid-binding proteins in vertebrate retina. J Cell Biol 97:703, 1983.
13. Lasansky A: Functional implications of structural findings in retinal glial cells. Prog Brain Res 15:48, 1965.
14. Rasmussen K-E: A morphometric study of the Müller cell cytoplasm in the rat retina. J Ultrastruct Res 39:413, 1972.
15. Rasmussen K-E: A morphometric study of the Müller cells, their nuclei and mitochondria, in the rat retina. J Ultrastruct Res 44:96, 1973.
16. Pedler C: The fine structure of the radial fibres in the reptile retina. Exp Eye Res 2:296, 1963.
17. Uga S, Smelser GK: Comparative study of the fine structure of retinal Müller cells in various vertebrates. Invest Ophthalmol 12:434, 1973.
18. Miller RF, Dowling JE: Intracellular responses of the Müller (glial) cells of mudpuppy retina: Their relation to b-wave of the electroretinogram. J Neurophysiol 33:323, 1970.
19. Reichenbach A, Hagen E, Schippel K, et al: Quantitative electron microscopy of rabbit Müller (glial) cells in dependence on retinal topography. Z Mikrosk-Anat Forsch 102:721, 1988.
20. Raviola G: The structural basis of the blood-ocular barriers. Exp Eye Res 25S:27, 1977.
21. Rasmussen K-E: The Müller cell: A comparative study of rod and cone retinas with and without retinal vessels. Exp Eye Res 19:243, 1974.
22. Mobbs P, Brew H, Attwell D: A quantitative analysis of glial cell coupling in the retina of the axolotl (Ambystoma mexicanum). Brain Res 460:235, 1988.
23. Conner JD, Detwiler PB, Sarthy PV: Ionic and electrophysiological properties of retinal Müller (glial) cells of the turtle. J Physiol 362:79, 1985.
24. Bunt-Milam AH, Saari JC, Klock IB, et al: Zonulae adherentes pore size in the external limiting membrane of the rabbit retina. Invest Ophthalmol Vis Sci 26:1377, 1985.
25. Ogden TE: Nerve fiber layer of the primate retina: thickness and glial content. Vision Res 23:581, 1983.
26. Hogan MJ, Alvarado JA, Weddell JE: Histology of the Human Eye. An Atlas and Textbook. Philadelphia, WB Saunders, 1971.
27. Kuwabara T: Blood vessels in the normal retina. *In* Straatsma BR, Hall MO, Allen RA, Crescitelli F (eds): The Retina: Morphology, Function and Clinical Characteristics. Berkeley, CA, University of California Press, 1969, pp 163–176.
28. Gotow T, Hashimoto PH: Orthogonal arrays of particles in plasma membranes of Müller cells in the guinea pig retina. Glia 2:273, 1989.
29. Richter W, Reichenbach A, Reichelt W: Orthogonal arrays of intramembraneous particles in the Müller cell and astrocyte endfoot membrane of rabbit retina. Postnatal development and adulthood. J Neurocytol 19:127, 1990.
30. Wolburg H, Berg K: Distribution of orthogonal arrays of particles in the Müller cell membrane of the mouse retina. Glia 1:246, 1988.
31. Reichenbach A, Wolburg H, Richter W, et al: Membrane ultrastructure preservation and membrane potentials after isolation of rabbit retinal glial (Müller) cells by papain. J Neurosci Meth 32:227, 1990.
32. Landis DMD, Reese TS: Arrays of particles in freeze-fractured astrocytic membranes. J Cell Biol 60:316, 1974.
33. Hatton JD, Ellisman MH: The distribution of orthogonal arrays and their relationship to intercellular junctions in neuroglia of the freeze-fractured hypothalamo-neurohypophysial system. Cell Tiss Res 215:309, 1981.
34. Kuwabara T, Cogan DG: Retinal glycogen. Arch Ophthalmol 66:680, 1961.
35. Chase J: The evolution of retinal vascularization in mammals. A comparison of vascular and avascular retinae. Ophthalmology 89:1518, 1982.
36. Eisenfeld AJ, Bunt-Milam AH, Saari JC: Localization of retinoid-binding proteins in developing rat retina. Exp Eye Res 41:299, 1985.
37. Bok D, Ong DE, Chytil F: Immunocytochemical localization of cellular retinol binding protein in the rat retina. Invest Ophthalmol Vis Sci 25:877, 1984.
38. Karwoski CJ, Proenza LM: Relationship between Müller cell responses, a local transretinal potential, and potassium flux. J Neurophysiol 40:244, 1977.
39. Newman EA: Distribution of potassium conductance in mammalian Müller (glial) cells: A comparative study. J Neurosci 7:2423, 1987.
40. Newman EA: Membrane physiology of retinal glial (Müller) cells. J Neurosci 5:2225, 1985.
41. Newman EA: Inward rectifying potassium channels in retinal glial (Müller) cells. Soc Neurosci Abstr 15:353, 1989.
42. Newman EA: Potassium conductance block by barium in amphibian Müller cells. Brain Res 498:308, 1989.
43. Brew H, Gray PTA, Mobbs P, et al: Endfeet of retinal glial cells have higher densities of ion channels that mediate K^+ buffering. Nature 324:466, 1986.
44. Newman EA: Inward-rectifying potassium channels in retinal Müller cells of the spiny dogfish (Squalus acanthias). Bull Mt Desert Island Biol Lab 29:104, 1990.
45. Newman EA: Regional specialization of retinal glial cell membrane. Nature 309:155, 1984.
46. Reichenbach A, Eberhardt W: Cytotopographical specialization of enzymatically isolated rabbit retinal Müller (glial) cells: K^+ conductivity of the cell membrane. Glia 1:191, 1988.
47. Newman EA: Voltage-dependent calcium and potassium channels in retinal glial cells. Nature 317:809, 1985.
48. Nilius B, Reichenbach A: Efficient K^+ buffering by mammalian retinal glial cells is due to cooperation of specialized ion channels. Pflugers Arch 411:654, 1988.
49. Puro DG, Roberge F, Chan C-C: Retinal glial cell proliferation and ion channels: A possible link. Invest Ophthalmol Vis Sci 30:521, 1989.
50. Dick E, Miller RF: Extracellular K^+ activity changes related to electroretinogram components. I. Amphibian (I-type) retinas. J Gen Physiol 85:885, 1985.
51. Dick E, Miller RF, Bloomfield S: Extracellular K^+ activity changes related to electroretinogram components. II. Rabbit (E-type) retinas. J Gen Physiol 85:911, 1985.
52. Newman EA, Astion ML: Localization and stoichiometry of electrogenic sodium-bicarbonate cotransport in retinal glial cells. Glia 4:424, 1991.
53. Newman EA: Electrogenic sodium-bicarbonate cotransport in retinal Müller cells of the spiny dogfish (Squalus acanthias). Bull Mt Desert Island Biol Lab 29:102, 1990.
54. Borgula GA, Karwoski CJ, Steinberg RH: Light-evoked changes in extracellular pH in frog retina. Vision Res 29:1069, 1989.
55. Oakley B II, Wen R: Extracellular pH in the isolated retina of the toad in darkness and during illumination. J Physiol 419:353, 1989.
56. Musser GL, Rosen S: Localization of carbonic anhydrase activity in the vertebrate retina. Exp Eye Res 15:105, 1973.
57. Linser PJ, Sorrentino M, Moscona AA: Cellular compartmentalization of carbonic anhydrase-C and glutamine synthetase in developing and mature mouse neural retina. Dev Brain Res 13:65, 1984.
58. Reichenbach A, Eberhardt W: Intracellular recordings from isolated rabbit retinal Müller (glial) cells. Pflugers Arch 407:348, 1986.
59. Reichenbach A, Hagen E, Schippel K, et al: Cytotopographical specialization of enzymatically isolated rabbit retinal Müller (glial) cells: Structure, ultrastructure, and 3H-ouabain binding sites. Z Mikrosk Anat Forsch 102:897, 1988.
60. Stirling CE, Sarthy PV: Localization of the Na-K pump in turtle retina. J Neurocytol 14:33, 1985.
61. Reichenbach A, Dettmer D, Reichelt W, et al: Na^+,K^+-activated adenosine triphosphatase of isolated Müller cells from the rabbit retina shows a K^+ dependence similar to that of brain astrocytes. Neurosci Lett 59:281, 1985.
62. McGrail KM, Sweadner KJ: Complex expression patterns for Na^+,K^+-ATPase isoforms in retina and optic nerve. Eur J Neurosci 2:170, 1989.
63. Brew H, Attwell D: Electrogenic glutamate uptake is a major current carrier in the membrane of axolotl retinal glial cells. Nature 327:707, 1987.

64. Henshel DS, Miller RF: Physiology and pharmacology of glutamate effects on dissociated Müller (glia) cells. Soc Neurosci [Abstract] 12:169, 1986.
65. Schwartz EA, Tachibana M: Electrophysiology of glutamate and sodium co-transport in a glial cell of the salamander retina. J Physiol 426:43, 1990.
66. Barbour B, Brew H, Attwell D: Electrogenic glutamate uptake in glial cells is activated by intracellular potassium. Nature 335:433, 1988.
67. Sarantis M, Attwell D: Glutamate uptake in mammalian retinal glia is voltage- and potassium-dependent. Brain Res 516:322, 1990.
68. Ehinger B: Glial and neuronal uptake of GABA, glutamic acid, glutamine and glutathione in the rabbit retina. Exp Eye Res 25:221, 1977.
69. Riepe RE, Norenburg MD: Müller cell localisation of glutamine synthetase in rat retina. Nature 268:654, 1977.
70. Sarthy PV, Lam DMK: Biochemical studies of isolated glial (Müller) cells from the turtle retina. J Cell Biol 78:675, 1978.
71. Hertz L, Schousboe A: Role of astrocytes in compartmentation of amino acid and energy metabolism. *In* Federoff S, Vernadakis A (eds): Astrocytes, vol 2. Orlando, FL, Academic Press, 1986, pp 179–208.
72. Sarthy PV: The uptake of [3H]gamma-aminobutyric acid by isolated glial (Müller) cells from the mouse retina. J Neurosci Meth 5:77, 1982.
73. Nishimura Y, Schwartz ML, Rakic P: Localization of gamma-aminobutyric acid and glutamic acid decarboxylase in rhesus monkey retina. Brain Res 359:351, 1985.
74. Malchow RP, Qian H, Ripps H: γ-Aminobutyric acid (GABA)–induced currents of skate Müller (glial) cells are mediated by neuronal-like GABAA receptors. Proc Natl Acad Sci USA 86:4326, 1989.
75. MacVicar BA, Tse FWY, Crichton SA, et al: GABA-activated Cl^- channels in astrocytes of hippocampal slices. J Neurosci 9:3577, 1989.
76. Oakley B II, Green DG: Correlation of light-induced changes in retinal extracellular potassium concentration with c-wave of the electroretinogram. J Neurophysiol 39:1117, 1976.
77. Karwoski CJ, Proenza LM: Light-evoked changes in extracellular potassium concentration in mudpuppy retina. Brain Res 142:515, 1978.
78. Kline RP, Ripps H, Dowling JE: Generation of b-wave currents in the skate retina. Proc Natl Acad Sci USA 75:5727, 1978.
79. Karwoski CJ, Proenza LM: Neurons, potassium, and glia in proximal retina of Necturus. J Gen Physiol 75:141, 1980.
80. Karwoski CJ, Newman EA, Shimazaki H, et al: Light-evoked increases in extracellular K^+ in the plexiform layers of amphibian retinas. J Gen Physiol 86:189, 1985.
81. Stockton RA, Slaughter MM: The b-wave of the electroretinogram: A reflection of ON bipolar cell activity. J Gen Physiol 93:101, 1989.
82. Fujimoto M, Tomita T: Reconstruction of the slow PIII from the rod potential. Invest Ophthalmol Vis Sci 18:1090, 1979.
83. Steinberg RH, Oakley BII, Niemeyer G: Light-evoked changes in $[K^+]_o$ in retina of intact cat eye. J Neurophysiol 44:897, 1980.
84. Newman EA: Regulation of potassium levels by glial cells in the retina. Trends NeuroSci 8:156, 1985.
85. Orkand RK, Nicholls JG, Kuffler SW: Effect of nerve impulses on the membrane potential of glial cells in the central nervous system of amphibia. J Neurophysiol 29:788, 1966.
86. Newman EA, Frambach DA, Odette LL: Control of extracellular potassium levels by retinal glial cell K^+ siphoning. Science 225:1174, 1984.
87. Eberhardt W, Reichenbach A: Spatial buffering of potassium by retinal Müller (glial) cells of various morphology calculated by a model. Neuroscience 22:687, 1987.
88. Immel J, Steinberg RH: Spatial buffering of K^+ by the retinal pigment epithelium in frog. J Neurosci 6:3197, 1986.
89. Karwoski CJ, Lu H-K, Newman EA: Spatial buffering of light-evoked potassium increases by retinal Müller (glial) cells. Science 244:578, 1989.
90. Faber DS: Analysis of Slow Transretinal Potentials in Response to Light. Buffalo, State University of New York, 1969. Thesis.
91. Newman EA: b-Wave currents in the frog retina. Vision Res 19:227, 1979.
92. Newman EA: Current source-density analysis of the b-wave of frog retina. J Neurophysiol 43:1355, 1980.
93. Heynen H, van Norren D: Origin of the electroretinogram in the intact macaque eye—II. Current source-density analysis. Vision Res 25:709, 1985.
94. Wen R, Oakley B II: K^+-evoked Müller cell depolarization generates b-wave of electroretinogram in toad retina. Proc Natl Acad Sci USA 87:2117, 1990.
95. Newman EA, Odette LL: Model of electroretinogram b-wave generation: A test of the K^+ hypothesis. J Neurophysiol 51:164, 1984.
96. Sieving PA, Frishman LA, Steinberg RH: M-wave of the proximal retina in cat. J Neurophysiol 56:1039, 1986.
97. Frishman LJ, Steinberg RH: Origin of negative potentials in the light-adapted ERG of the cat retina. J Neurophysiol 63:1333, 1990.
98. Steinberg RH, Frishman LJ, Sieving PA: Negative components of the electroretinogram from proximal retina and photoreceptor. Prog Retinal Res 10:121, 1991.
99. Sieving PA, Frishman LR, Steinberg RH: Scotopic threshold response of proximal retina in cat. J Neurophysiol 56:1049, 1986.
100. Frishman LJ, Steinberg RH: Light-evoked increases in $[K^+]_o$ in proximal portion of the dark-adapted cat retina. J Neurophysiol 61:1233, 1989.
101. Frishman LJ, Steinberg RH: Intraretinal analysis of the threshold dark-adapted ERG of cat retina. J Neurophysiol 61:1221, 1989.
102. Sieving PA, Nino C: Scotopic threshold response (STR) of the human electroretinogram. Invest Ophthalmol Vis Sci 29:1608, 1988.
103. Sieving PA: Retinal ganglion cell loss does not abolish the scotopic threshold response (STR) of the cat and human ERG. Clin Vision Sci 6:149, 1991.
104. Witkovsky P, Dudek FE, Ripps H: Slow PIII component of the carp electroretinogram. J Gen Physiol 65:119, 1975.
105. Matsuura T: Effects of barium on separately recorded fast and slow PIII responses in bullfrog retina. Experientia 40:817, 1984.
106. Bolnick DA, Walter AE, Sillman AJ: Barium suppresses slow PIII in perfused bullfrog retina. Vision Res 19:1117, 1979.
107. Lurie M, Marmor MF: Similarities between the c-wave and slow PIII in the rabbit eye. Invest Ophthalmol Vis Sci 19:1113, 1980.
108. Cohen A: A possible cytological basis for the 'R' membrane in the vertebrate eye. Nature 205:1222, 1965.
109. Steinberg RH, Wood I: Pigment epithelial cell ensheathment of cone outer segments in the retina of the domestic cat. Proc R Soc Lond (Biol) 187:461, 1974.
110. Fisher SK, Steinberg RH: Origin and organization of pigment epithelial apical projections to cones in cat retina. J Comp Neurol 206:131, 1982.
111. Lasansky A, DeFisch FW: Potential, current, and ionic fluxes across the isolated retinal pigment epithelium and chloroid. J Gen Physiol 49:913, 1966.
112. Miller SS, Steinberg RH: Active transport of ions across frog retinal pigment epithelium. Exp Eye Res 25:235, 1977.
113. Miller SS, Steinberg RH, Oakley BII: The electrogenic sodium pump of the frog retinal pigment epithelium. J Membrane Biol 44:259, 1978.
114. Brown KT, Wiesel TN: Localization of electrical activity in the cat retina by an electrode marking method. J Physiol 158:281, 1961.
115. Joseph DP, Miller SS: Apical and basal membrane ion transport mechanisms in bovine retinal pigment epithelium. J Physiol 435:439, 1991.
116. Hughes BA, Steinberg RH: Voltage-dependent currents in isolated cells of the frog retinal pigment epithelium. J Physiol 428:273, 1990.
117. Wen R, Lui GM, Steinberg RH: Voltage-dependent whole cell currents in cultured human and monkey RPE cells. Invest Ophthalmol Vis Sci 32:671, 1991.
118. Fox JA, Pfeffer BA, Fain GL: Single-channel recordings from cultured human retinal pigment epithelium cells. J Gen Physiol 91:193, 1988.
119. Miller SS, Edelman JL: Active ion transport pathways in the bovine retinal pigment epithelium. J Physiol 424:283, 1990.
120. Miller SS, Steinberg RH: Potassium transport across the frog retinal pigment epithelium. J Membrane Biol 67:199, 1982.
121. Oakley B II, Miller SS, Steinberg RH: Effect of intracellular

potassium upon the electrogenic pump of frog retinal pigment epithelium. J Membrane Biol 44:281, 1978.
122. Frambach DA, Misfeldt DS: Furosemide-sensitive Cl transport in embryonic chicken retinal pigment epithelium. Am J Physiol 244:F679, 1983.
123. Kennedy BG: Na^+-K^+-Cl^- cotransport in cultured cells derived from human retinal pigment epithelium. Am J Physiol 259:C29, 1990.
124. Adorante JS, Miller SS: Potassium-dependent volume regulation in retinal pigment epithelium is mediated by Na,K,Cl transport. J Gen Physiol 96:1153, 1990.
125. Gallemore RP, Steinberg RH: Effects of DIDS on the chick retinal pigment epithelium. I. Membrane potentials, apparent resistances, and mechanisms. J Neurosci 9:1968, 1989.
126. LaCour M, Lund-Anderson H, Zeuthen T: Potassium transport of the frog retinal pigment epithelium: Autoregulation of potassium activity in the subretinal space. J Physiol 375:461, 1986.
127. Hughes BA, Adorante JS, Miller SS, et al: Apical electrogenic $NaHCO_3$ cotransport. A mechanism for HCO_3 absorption across the retinal pigment epithelium. J Gen Physiol 94:125, 1989.
128. LaCour M: Rheogenic sodium-bicarbonate co-transport across the retinal membrane of the frog retinal pigment epithelium. J Physiol 419:539, 1989.
129. Lin H, Miller SS: pHi regulation in frog retinal pigment epithelium: two apical membrane mechanisms. Am J Physiol 261:C132, 1991.
130. Fujii S, Gallemore RP, Hughes BA, et al: Direct evidence for a basolateral membrane Cl^- conductance in the toad retinal pigment epithelium. Am J Physiol 262:C374, 1992.
131. Miller SS, Steinberg RH: Passive ionic properties of frog retinal pigment epithelium. J Membrane Biol 36:337, 1977.
132. Fong CN, Bialek S, Hughes BA, et al: Modulation of intracellular chloride in bullfrog retinal pigment epithelium. FASEB J 2(A):1722, 1988.
133. Marmor MF: Control of subretinal fluid: Experimental and clinical studies. Eye 4:340, 1990.
134. Hughes BA, Miller SS, Machen TE: Effects of cyclic AMP on fluid absorption and ion transport across frog retinal pigment epithelium. Measurements in the open-circuit state. J Gen Physiol 83:875, 1984.
135. Joseph DP, Miller SS: Alpha-adrenergic receptors mediate basal membrane voltage and resistance changes in bovine retinal pigment epithelium (RPE). Invest Ophthalmol Vis Sci 29(Suppl):20, 1988.
136. Joseph DP, Miller SS: Alpha-adrenergic receptor activation at bovine RPE apical membrane affects basolateral membrane Cl channels. Invest Ophthalmol Vis Sci 30(Suppl):413, 1989.
137. Edelman JL, Miller SS: Epinephrine stimulates fluid absorption across retinal pigment epithelium. Invest Ophthalmol Vis Sci 31(Suppl):70, 1990.
138. Dawis SM, Niemeyer G: Similarity and diversity of monoamines in their effects on the standing potential, light peak and electroretinogram of the perfused cat eye. Clin Vision Sci 3:109, 1988.
139. Frambach DA, Fain GL, Farber DB, et al: Beta adrenergic receptors on cultured human retinal pigment epithelium. Invest Ophthalmol Vis Sci 31:1767, 1990.
140. Frambach DA, Valentine JL, Weiter JJ: Alpha-1 adrenergic receptors on rabbit retinal pigment epithelium. Invest Ophthalmol Vis Sci 29:737, 1988.
141. Dearry A, Burnside B: Dopamine induces light-adaptive retinomotor movements in teleost photoreceptors and retinal pigment epithelium. *In* Liss AR (ed): Dopaminergic Mechanisms in Vision. New York, AR Liss, 1988, pp 109–135.
142. Gallemore RP, Steinberg RH: Effects of dopamine on the chick retinal pigment epithelium. Invest Ophthalmol Vis Sci 31:67, 1990.
143. Nao-i N, Nilsson SEG, Gallemore RP, et al: Effects of melatonin on the chick retinal pigment epithelium: Membrane potentials and light-evoked responses. Exp Eye Res 49:573, 1989.
144. Miller SS, Hughes BA, Machen TE: Fluid transport across retinal pigment epithelium is inhibited by cyclic AMP. Proc Natl Acad Sci USA 79:2111, 1982.
145. Miller SS, Farber D: Cyclic AMP modulation of ion transport across frog retinal pigment epithelium. Measurements in the short-circuit state. J Gen Physiol 83:853, 1984.
146. Hughes BA, Miller SS, Joseph DP, et al: cAMP stimulates the Na^+-K^+ pump in frog retinal pigment epithelium. Am J Physiol 254:C84, 1988.
147. Nao-i N, Gallemore RP, Steinberg RH: Effects of cAMP and IBMX on the chick retinal pigment epithelium. Invest Ophthalmol Vis Sci 31:54, 1990.
148. Steinberg RH, Schmidt R, Brown KT: Intracellular responses to light from cat pigment epithelium: Origin of the electroretinogram c-wave. Nature 227:728, 1970.
149. Oakley B II, Steinberg RH, Miller SS, et al: The in vitro frog pigment epithelial cell hyperpolarization in response to light. Invest Ophthalmol Vis Sci 16:771, 1977.
150. Oakley B II: Potassium and the photoreceptor-dependent pigment epithelial hyperpolarization. J Gen Physiol 70:405, 1977.
151. Gardner-Medwin AR: Analysis of potassium dynamics in mammalian brain tissue. J Physiol 335:393, 1983.
152. Linsenmeier RA, Steinberg RH: Variations of c-wave amplitude in the cat eye. Doc Ophthalmol Proc Ser 37:21, 1983.
153. Linsenmeier RA, Steinberg RH: Delayed basal hyperpolarization of cat retinal pigment epithelium and its relation to the fast oscillation of the DC electroretinogram. J Gen Physiol 83:213, 1984.
154. Griff ER, Linsenmeier RA, Steinberg RH: The cellular origin of the fast oscillation. Doc Ophthalmol Proc Ser 37:13, 1983.
155. Griff ER, Steinberg RH: Changes in apical $[K^+]$ produce delayed basal membrane responses of the retinal pigment epithelium in the gecko. J Gen Physiol 83:193, 1984.
156. Gallemore RP, Steinberg RH: Effects of DIDS on the chick retinal pigment epithelium. II. Mechanism of the light peak and other responses originating at the basal membrane. J Neurosci 9:1977, 1989.
157. Fujii S, Hughes BA, Steinberg RH: Effects of current clamp on chick retinal pigment epithelium. Invest Ophthalmol Vis Sci 32:2047, 1991.
158. Rabin J, Adams AJ, McCray PB Jr, et al: Evidence for an abnormal Cl transport in the retinal pigment epithelium of CF patients. Pediatr Pulmonol 5(Suppl):290, 1990.
159. Steinberg RH, Griff ER, Linsenmeier RA: The cellular origin of the light peak. Doc Ophthalmol Proc Ser 37:1, 1983.
160. Rudolf G, Wioland N, Kempf E, et al: Electrooculographic study in the chicken after treatment with neurotoxin 6-hydroxydopamine. Doc Ophthalmol 72:83, 1989.
161. Wioland N, Rudolf G, Bonaventure N: Electrooculographic and electroretinographic study in the chicken after dopamine and haloperidol. Doc Ophthalmol 75:175, 1990.
162. Linsenmeier RA, Steinberg RH: Mechanisms of hypoxic effects on the cat DC electroretinogram. Invest Ophthalmol Vis Sci 27:1385, 1986.
163. Linsenmeier RA, Steinberg RH: Mechanisms of azide induced increases in the c-wave and standing potential of the intact cat eye. Vision Res 27:1, 1987.
164. Marmor MF, Donovan WJ, Gaba DM: Effects of hypoxia and hyperoxia on the human standing potential. Doc Ophthalmol 60:347, 1985.
165. Young RW: Visual cells, daily rhythms, and vision research. Vision Res 18:573, 1978.
166. Young RW: Visual cells and the concept of renewal. Invest Ophthalmol Vis Sci 15:700, 1976.
167. Long KO, Fisher SK, Fariss RN, et al: Disc shedding and autophagy in the cone-dominant ground squirrel retina. Exp Eye Res 43:193, 1986.
168. Feeny-Burns L, Hilderbrand ES, Eldridge S: Aging human RPE: morphometric analysis of macular, equatorial, and peripheral cells. Invest Ophthalmol Vis Sci 25:195, 1984.
169. van Horn D, Aaberg TM: Pigment epithelial proliferation in human retinal detachment with massive periretinal proliferation. Am J Ophthalmol 85:181, 1978.
170. Machemer R, Laqua H: Pigment epithelium proliferation in retinal detachment (massive periretinal proliferation). Am J Ophthalmol 80:1, 1975.
171. Algvere P, Kock E: Experimental epiretinal membranes induced by intravitreal carbon particles. Am J Ophthalmol 96:345, 1983.
172. Steinberg RH: Research update: Report from a workshop on cell biology of retinal detachment. Exp Eye Res 43:695, 1986.
173. Mullen RJ, LaVail MM: Inherited retinal dystrophy: primary defect in pigment epithelium determined with experimental rat chimeras. Science 192:799, 1976.

174. Li L, Turner JE: Inherited retinal dystrophy in the RCS rat: prevention of photoreceptor degeneration by pigment epithelial cell transplantation. Exp Eye Res 47:911, 1988.
175. Lopez R, Gouras P, Kjeldbye H, et al: Transplanted retinal pigment epithelium modifies the retinal degeneration in the RCS rat. Invest Ophthalmol Vis Sci 30:586, 1989.
176. Faktorovich EG, Steinberg RH, Yasumura D, et al: Photoreceptor degeneration in inherited retinal dystrophy delayed by basic fibroblast growth factor. Nature 347:83, 1990.
177. Schweigerer L, Malerstein B, Neufeld G, et al: Basic fibroblast growth factor is synthesized in cultured retinal pigment epithelial cells. Biochem Biophys Res Commun 143:934, 1987.
178. Sternfeld MD, Robertson JE, Shipley GD, et al: Cultured human retinal pigment epithelial cells express basic fibroblast growth factor and its receptor. Current Eye Res 8:1029, 1989.
179. Ramon y Cajal S: The Structure of the Retina. Springfield, IL: Charles C Thomas, 1972.

Chapter 25

Origins of Field Potentials

MICHAEL A. SANDBERG

INTRODUCTION

This chapter summarizes current knowledge concerning the physiologic bases of light-evoked and pattern-evoked field potentials that may be recorded from patients with visual loss to help localize the source of malfunction and quantify its extent. The field potentials considered include the early receptor potential, the electrooculogram, the flash and pattern electroretinograms, and the pattern visual-evoked response. The evidence and conclusions cited here derive primarily from recordings in animals obtained with microelectrodes, after pharmacologic treatment, or after surgery and in patients with known anatomic lesions of the visual pathways. Details for eliciting, recording, and interpreting these responses with respect to the diagnosis or quantification of disease of the visual pathways are considered elsewhere (*Principles and Practice of Ophthalmology: Clinical Practice,* Chapters 104 to 108).

GENERAL CONSIDERATIONS

Field potentials are time varying electrical activity recorded at some location external and generally remote to the source of generation. Biologic field potentials, such as the electroretinogram or visual-evoked response, may be recorded on the surface of the organism so that there is no risk from invasive procedures to the patient or animal and no possibility that the monitoring electrode will itself disturb the physiologic integrity of the generator; for some measurements, the organism may be free to move about its environment. These potentials may be endogenous (in part), occurring at times to variable degree without the need of an external stimulus. An example is the standing potential of the eye that has a small-amplitude slow oscillation that is triggered by light but persists even after the eye has been in extended darkness. In most cases, however, biologic field potentials require some external stimulus for each response. For the eye, the optimal stimulus is light; but pressure, magnetism, and electricity are also effective and lead to vision.

Biologic field potentials are carried by volume conduction through ionic (i.e., salt) solutions and attenuated to large or small degree by structures of high or low resistance, respectively, to ionic flow. In response to an effective stimulus, a neuron (e.g., a retinal bipolar cell) is an active "source" of current that exits the cell at some location and flows through the extracellular space. This current reenters the cell at some other location, known as the current "sink." The current is strongest in the vicinity of the cell (e.g., within the retina), weaker at a small distance (e.g., within the vitreous humor), and weaker yet at a large distance (e.g., at the cornea). Glial (e.g., Müller) cells may act as sources and sinks of current if they have a high concentration gradient and permeability to an ion (e.g., K^+) whose concentration changes in the extracellular space owing to neural activity. If these current sources and sinks are oriented radially as dipoles with respect to the monitoring electrodes, then they will register a time-varying voltage change. Retinal pigment epithelial cells, photoreceptor cells, bipolar cells, and Müller cells all act as radially oriented dipoles with respect to a vitreal or corneal electrode and, thus, contribute to the electroretinogram. Horizontal and possibly amacrine cells have their dipoles oriented tangentially to these electrodes and appear not to contribute independently to the electroretinogram.

Because field potentials are often recorded at some appreciable distance from the source and cross barriers of significant resistance, current (or voltage) is necessarily smaller than that recorded in close proximity to or within the generator. For example, responses from single photoreceptors to light flashes may be tens of millivolts in amplitude when monitored intracellularly with a microelectrode but only some hundreds of microvolts from the entire retina when monitored at the cornea with a contact lens electrode. However, with contem-